Vol. 729: 1–29, 2024
https://doi.org/10.3354/meps14531

MARINE ECOLOGY PROGRESS SERIES
Mar Ecol Prog Ser

Published February 22

FEATURE ARTICLE

From land to sea: the fall migration of the red phalarope through the Western Hemisphere

Sarah T. Saalfeld[1,*], Mihai Valcu[2], Stephen Brown[3], Willow English[4], Marie-Andrée Giroux[5], Autumn-Lynn Harrison[6], Johannes Krietsch[2], Kathy Kuletz[1], Jean-François Lamarre[7], Christopher Latty[8], Nicolas Lecomte[9], Rebecca McGuire[10], Martin Robards[10], Amy Scarpignato[6], Shiloh Schulte[3], Paul A. Smith[11], Bart Kempenaers[2], Richard B. Lanctot[1]

[1]Migratory Bird Management Division, US Fish and Wildlife Service, Anchorage, Alaska 99503, USA

Full author addresses are given in Appendix A

ABSTRACT: Understanding how and where individuals migrate between breeding and wintering areas is important for assessing threats, identifying important areas for conservation, and determining a species' vulnerability to changing environmental conditions. Between 2017 and 2020, we tracked post-breeding movements of 72 red phalaropes *Phalaropus fulicarius* with satellite tags from 7 Arctic-breeding sites in the Alaskan and Central Canadian Arctic. All tracked red phalaropes left their Arctic breeding grounds (i.e. were obligate migrants) but then switched to a more facultative migration strategy with a fly-and-forage migration pattern once in the marine environment. We documented high variability in migration timing and routes, with birds often taking indirect, circuitous routes with numerous stops that greatly lengthened both the duration and distance of their southward migration. Across nearly 500 stopover areas, which were often associated with areas of presumed greater food availability, individuals spent an average of 6 d and traveled within an average area of 1880 km^2. Stopover areas were concentrated in onshore and nearshore habitats of the Beaufort and Chukchi seas, the western edge of the Bering Strait, along the Alaska Peninsula and Aleutian Islands, and near the Pribilof Islands in Alaska. Within the Beaufort and Chukchi seas, females frequently stopped within the marginal ice zone, whereas males tended to stay on land or in open water. Our results identified important marine areas that can aid future conservation and management decisions. However, conservation of the species will also need to address the numerous direct and indirect anthropogenic threats red phalaropes experience at sea, many of which are not site-specific.

*Corresponding author: sarah_saalfeld@fws.gov

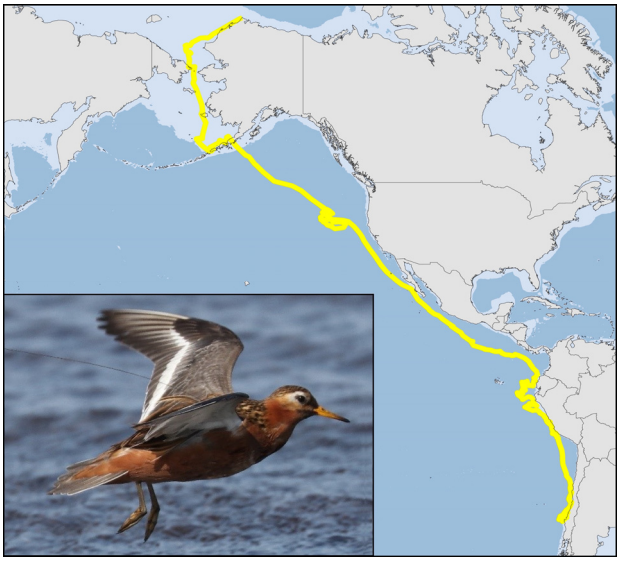

Individual example of red phalarope migration from tundra to marine habitats.

Photo: Manomet/Shiloh Schulte, Map: USFWS/Sarah Saalfeld

KEY WORDS: *Phalaropus fulicarius* · Animal tracking · Beringia · Bering Sea · Chukchi Sea · PTT tags · Shorebirds · Seabirds

1. INTRODUCTION

Many bird species migrate between breeding and wintering areas each year. Benefits of migration include avoiding exposure to severe weather and in-

Publisher: Inter-Research · www.int-res.com

creasing access to food (Herrera 1978, Newton & Dale 1996, Somveille et al. 2015), as well as reducing risk to predation (Gilg & Yoccoz 2010, McKinnon et al. 2010) or parasites (Piersma 1997), and reducing competition with individuals of the same or different species (Newton 2008). However, migration is not without its risks, especially for long-distance migrants that face a variety of threats at numerous locations throughout their annual cycle. As a result, many long-distance migrants have shown greater population declines when compared to resident or short-distance migrants (Both et al. 2010).

In addition to migratory distance, how a bird makes its way between breeding and wintering areas may impact its vulnerability, and species appear to have evolved several strategies to successfully complete migration. For example, many species that migrate through areas with predictable habitats or food availability have adopted an obligate migration strategy where the timing and direction of their migration, as well as the location of their breeding and wintering areas (i.e. site fidelity), is highly consistent among years and individuals (Newton 2012). On the other end of the spectrum, many species with unpredictable habitats or food availability have adopted a facultative migration strategy with highly variable migration patterns and low site fidelity, allowing individuals to respond to annual changes in resource availability by altering their behavior (Newton 2012). While long-distance migrants tend to have an obligate migration strategy and short-distance, dispersive, or irruptive migrants tend to have a facultative migration strategy, others can have traits of both or switch between modes during migration (Newton 2012). Thus, understanding variation in migration strategies among individuals and species is an important first step in determining the vulnerability of species to changing environmental conditions.

One group of birds that may be particularly vulnerable during migration are long-distance migratory seabirds. This is because many seabirds exhibit a fly-and-forage migration pattern in which they regularly stop to forage within the pelagic environment as they make their way from breeding to wintering areas (Amélineau et al. 2021). However, given the highly dynamic nature of the pelagic environment, the reliability of finding foraging opportunities during migration can vary both within and across seasons. For example, planktivorous seabirds that reside in the nearshore and pelagic environment forage opportunistically on zooplankton such as copepods (e.g. *Calanus* spp.), amphipods, fish eggs, and fish larvae. However, the availability of zooplankton can be highly unpredictable, as it is controlled by numerous variables, including climate (e.g. temperature and wind), physical oceanographic (e.g. salinity, sea surface temperature, currents, upwellings, and extent and timing of sea ice retreat) and biological factors (e.g. phytoplankton biomass and whale abundance; reviewed in Hopcroft et al. 2008, Smith et al. 2017). Thus, prey availability is likely to influence seabird movements during migration, determining where and when individuals stop (Amélineau et al. 2021).

To add to this unpredictability, many of these processes are changing rapidly and dramatically by global climate change caused by anthropogenic fossil fuel emissions, especially in the Arctic. For example, across the Arctic Ocean, sea surface temperatures in August have increased by an estimated 1°C per decade from 1982–2020 (Timmermans & Labe 2020). Concurrently, sea ice extent in September has been reduced by an average of 84% in the Eastern Siberian, Chukchi, and Beaufort seas, resulting in a combined total of 1.9 million km^2 of summer sea ice loss from 1979–2018, with the Chukchi Sea now remaining ice-free during the summer (Stroeve & Notz 2018). Such dramatic increases in sea surface temperatures and reduction in sea ice extent are resulting in a cascade of events, from seasonal changes in primary production (e.g. the amount of phytoplankton produced, as well as the timing of phytoplankton blooms) to changes in the distribution and composition of a whole host of species (e.g. zooplankton, fish, seabirds, and marine mammals) across the food web (Overland & Stabeno 2004, Grebmeier et al. 2006, Cusset et al. 2019, Duffy-Anderson et al. 2019, Stevenson & Lauth 2019, Huntington et al. 2020). In addition, warmer sea surface temperatures are predicted to lead to a higher frequency of toxic algal blooms (Glibert et al. 2014, Gibble & Hoover 2018, Huntington et al. 2020), which, when combined with changes in food-web dynamics, have been associated with mortality events of both piscivorous and planktivorous seabirds (Jones et al. 2018, 2023, Van Hemert et al. 2020, 2021).

In addition to climatic changes, seabirds also face other anthropogenic threats including the ingestion of plastics, especially microplastics that float on the surface (Moser & Lee 1992, Drever et al. 2018, Baak et al. 2020, Flemming et al. 2022), increased vessel traffic that can result in disturbance and collisions (CAFF 2017), disorientation and fatal attraction to lights produced by ocean vessels and developments (Merkel 2010, Gjerdrum et al. 2021), the release of contaminants from marine vessels and oil and gas developments and their associated activities (Tyler et al. 1993,

Wahl et al. 1993, O'Hara & Morandin 2010), and disturbance, displacement, and collisions with offshore wind farms (Garthe & Hüppop 2004, Stienen et al. 2007, Furness et al. 2013, Dierschke et al. 2016).

The red phalarope *Phalaropus fulicarius*, while technically classified as a shorebird, functionally acts like a surface-feeding, planktivorous seabird during the nonbreeding season and is thus likely affected by the threats listed above. However, little is known about the species' migratory routes, stopover areas, or connectivity between breeding and wintering areas (Hunnewell et al. 2016, Tracy et al. 2020). During the breeding season, red phalaropes spend 1–2 mo nesting in coastal tundra habitat of the Holarctic, exhibiting social polyandry with sex-role reversal in which females sequentially mate with multiple males and only males incubate eggs and care for offspring (van Bemmelen 2019, Tracy et al. 2020, Krietsch et al. 2022). After the breeding season, red phalaropes, especially juveniles, are regularly observed in nearshore habitats of the Beaufort and Chukchi seas (Connors et al. 1981, Smith & Connors 1993, Andres 1994, Taylor et al. 2010, 2011), with females generally arriving in these habitats earlier than males (Connors et al. 1981). Red phalaropes then enter the pelagic environment, with some wintering in the Pacific Ocean (primarily off the coast of Peru and Chile, but occasionally as far north as northern California) and others in the Atlantic Ocean (from southern North Carolina to the Caribbean; Tracy et al. 2020). Thus, there are likely 2 populations of red phalaropes in North America, although the location of the geographic divide that separates these 2 populations remains unknown (Tracy et al. 2020). While in the pelagic environment, red phalaropes are often in areas far (e.g. 80–160 km) from the coast (Briggs et al. 1984, Brown & Gaskin 1988, Vermeer et al. 1993, Tracy et al. 2020), where prey concentrates near the surface such as at ocean fronts (i.e. convergent water masses where temperature and salinity change abruptly) or upwellings (Briggs et al. 1984, Brown & Gaskin 1988, DiGiacomo et al. 2002). Red phalaropes also forage near grounded sea ice or in areas of low (e.g. <40%) sea-ice concentration (Divoky 1979, Connors et al. 1981, Orr et al. 1982), as well as near whales whose foraging behavior brings zooplankton to the surface (Nelson 1883, Obst & Hunt 1990, Grebmeier & Harrison 1992, Elphick & Hunt 1993).

To better understand how this species migrates, detailed movement data are needed. Taylor et al. (2011) tracked red phalaropes using very high frequency (VHF) radio tags and land- and aerial-based detection platforms in the Alaskan Arctic, but despite tremendous effort, relocated only 5 of 69 tagged individuals, each only once at nearby (<150 km from capture site) coastal sites within the Arctic. van Bemmelen (2019) tracked 16 red phalaropes from breeding sites in Greenland and Svalbard to wintering areas in the Atlantic Ocean using light-level geolocators, documenting southward movements of the Atlantic population. However, no study to date has tracked the southward migration of the Pacific population of red phalaropes breeding in North America, and neither the Atlantic nor Pacific population has been tracked with devices capable of high spatial resolution. As recent evidence suggests that red phalaropes are declining (Gratto-Trevor et al. 1998, Gall et al. 2017, Alaska Shorebird Group 2019, Smith et al. 2020, B. McCaffery unpubl. data), likely due to threats during the nonbreeding season when they switch to a marine lifestyle (Weiser et al. 2018a), it is important to understand the migratory movements of red phalaropes and the physical and ecological factors experienced by them while at sea.

In this study, we used satellite tags to track the migratory movements of male and female red phalaropes from their breeding sites in the Alaskan and Central Canadian Arctic. Our objectives were to (1) describe migration routes and stopover areas of individual birds, (2) identify important areas used by the population, and (3) relate this information to oceanographic conditions. We were especially interested in understanding the use of Arctic waters given the accelerated climatic changes that are affecting sea ice extent in this region (Callaghan et al. 2005, Serreze & Francis 2006, Hodgkins 2014, Notz & Stroeve 2016, Wang et al. 2018). Based on prior studies summarized above, we made the following predictions: (1) females would leave Arctic-breeding sites earlier than males, as only males incubate eggs and care for offspring; (2) adults from both populations would use coastal areas post-breeding before migrating into the pelagic environment; (3) adults would migrate along 2 distinct migration routes, with birds breeding in the Alaskan Arctic traveling toward the Pacific Ocean to winter off the coast of Central and South America, and birds breeding in the Central Canadian Arctic traveling toward the Atlantic Ocean to winter off the coast of the eastern United States or Africa; and (4) once in the marine environment, individuals would occur far from the coast in association with areas of greater food availability such as in highly productive ocean currents, near ocean fronts or upwellings, or in association with the marginal ice zone.

2. MATERIALS AND METHODS

2.1. Capture and nest monitoring

We captured 72 female red phalaropes during pre-breeding by dropping a mist net on them while they foraged in or along the edges of shallow ponds in late May–early June at Utqiaġvik, Alaska, USA, in 2017 and 2018 (Table 1, Fig. 1). We captured 31 incubating males on their nest using a bow-net (Priklonsky 1960) in late June–early July at 7 sites across the Arctic in 2019 and 2020 (Table 1, Fig. 1). We found nests by opportunistically flushing adults, or by following adults back to their nests after spotting them during systematic area searches or while dragging a rope across the tundra (Saalfeld & Lanctot 2015). Upon capture, we marked each individual with a US Geological Survey metal leg band and attached a 2 g solar-powered Argos platform transmitter terminal (PTT) tag (Microwave Telemetry) with either (1) a full-body harness (Chan et al. 2016) made of either 1.9 mm diameter Teflon held together with 3 crimps (2017) or 1.0 mm (outer diameter) silicone surgical tubing with knots (2018–2020) or (2) glue on the back approximately 1 cm above the uropygial gland after feather clipping (only at East Bay field site in 2019; Warnock & Warnock 1993). Attaching the tag on the upper back ensured that the solar panel received sunlight, so the battery remained charged. Tags weighed, on average, 3.4% (range = 2.7–4.1%) of the females' body mass and 4.0% (range = 3.4–5.0%) of the males' body mass.

We revisited the nests of most tagged males to assess tag attachment and to determine nest attendance and fate. We also visited nests found with fewer than 4 eggs (modal clutch size) 1 to 2 additional times until the clutch was completed, or until the clutch size remained unchanged for 2 consecutive days. We estimated nest initiation dates (i.e. date first egg laid) assuming 1 egg was laid per day. For nests found during incubation, we floated eggs in water to estimate the start of incubation (i.e. date 4th egg laid; Liebezeit et al. 2007). We predicted hatch date by adding 19 d (incubation period for this species; Weiser et al. 2018b) to the estimated incubation start date (Day 0 = date last egg laid). We checked nests approximately every 5 d until 3–4 d prior to the estimated hatch date, at which time we checked nests every 2 d until eggs were starred (i.e. hatching was initiated), and daily thereafter. We defined a nest as successful when at least 1 egg hatched (Mayfield 1975). See Saalfeld & Lanctot (2015) for evidence used to determine hatching or failure. When the evidence at the nest was not conclusive, we classified the nest fate as unknown.

2.2. Tracking movements

Location data from PTT tags deployed on birds were estimated via the Argos satellite system (by measuring the Doppler effect on transmission frequency) and included point locations and estimated errors (Douglas et al. 2012, Lopez et al. 2014). Because gaps in transmissions occurred at unpredictable intervals (e.g. due to low battery or poor satellite coverage), we standardized location data by estimating 1 location every 8 h by fitting a continuous-time random walk state-space model to each individual's locations using the 'foieGras' package (Jonsen et al. 2019, 2020, Jonsen & Patterson 2020) in R (R Core Team 2021). This approach accounts for the error associated with each location (as estimated by the location quality class) while predicting locations at regular intervals. We chose an 8 h time interval to estimate several locations per day while avoiding model overfit (i.e. predicting locations when there were large temporal data gaps; ~14% of predicted

Table 1. Capture location, year, and number of female and male red phalaropes equipped (parentheses indicate number tracked post-breeding) with 2 g solar-powered Argos platform transmitter terminal (PTT) tags from 2017–2020

Capture location	State/Province	Country	Latitude	Longitude	Year	Female	Male
Utqiaġvik	Alaska	USA	71.273	−156.614	2017	41 (28)	
Utqiaġvik	Alaska	USA	71.273	−156.614	2018	31 (22)	
Utqiaġvik	Alaska	USA	71.273	−156.614	2019		5 (4)
Utqiaġvik	Alaska	USA	71.273	−156.614	2020		10 (7)
Qupaluk	Alaska	USA	70.673	−152.845	2019		3 (2)
Colville River	Alaska	USA	70.438	−150.688	2019		1 (1)
Canning River	Alaska	USA	70.117	−145.838	2019		3 (3)
Cambridge Bay	Nunavut	Canada	69.171	−105.117	2019		1 (0)
East Bay	Nunavut	Canada	63.979	−81.702	2019		4 (2)
Igloolik	Nunavut	Canada	69.392	−81.566	2019		4 (3)

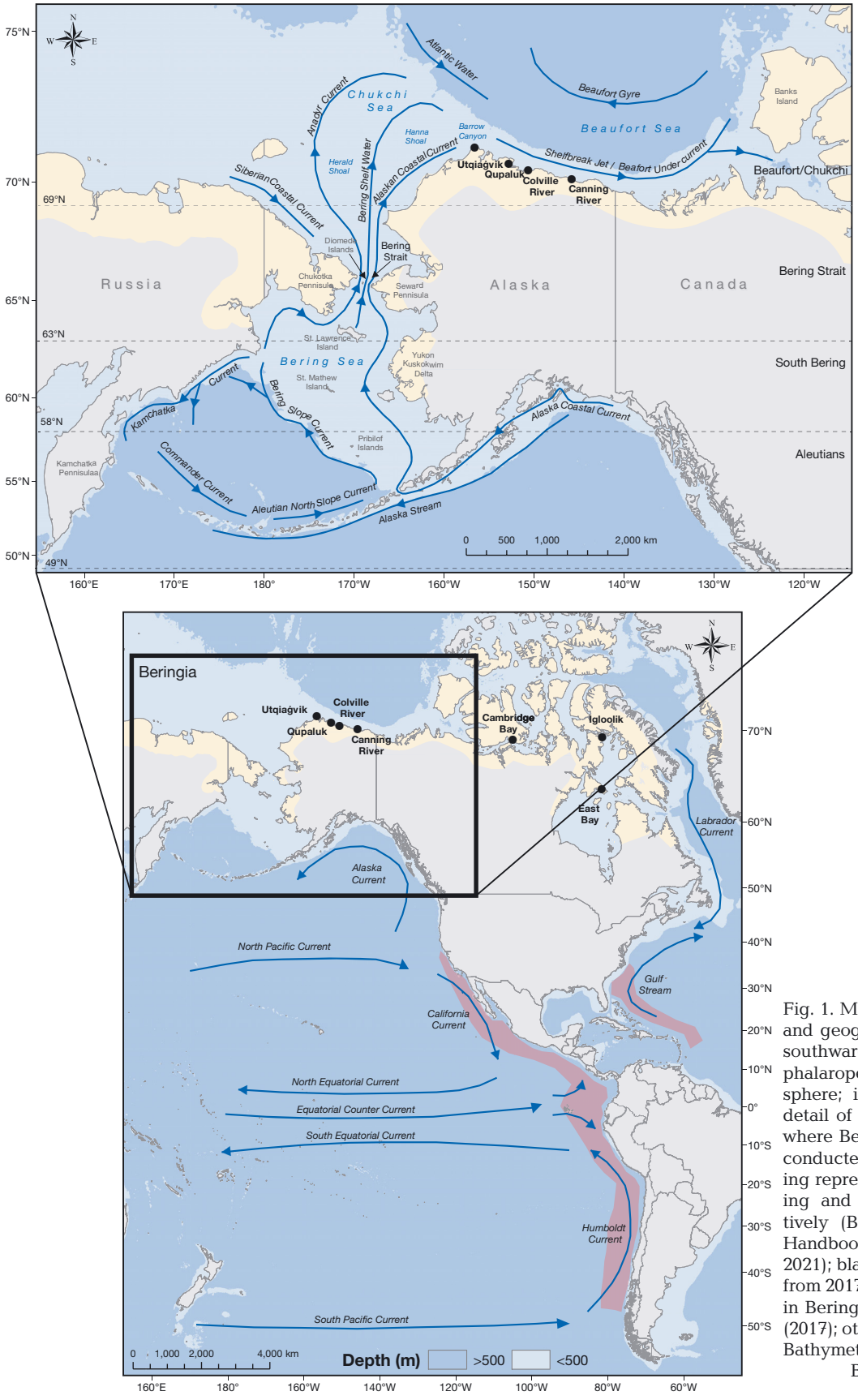

Fig. 1. Major currents, bathymetry, and geographic features along the southward migration route of red phalaropes in the Western Hemisphere; inset map provides more detail of features in Beringia (area where Beringia-only analyses were conducted). Yellow and pink shading represent red phalarope breeding and wintering areas, respectively (BirdLife International and Handbook of the Birds of the World 2021); black dots: tagging locations from 2017–2020 (Table 1). Currents in Beringia taken from Smith et al. (2017); others from Pidwirny (2006). Bathymetry (blue shading) from Becker et al. (2009)

locations occurred when temporal data gaps were >8 h). We calculated geodesic distances between consecutive 8 h predicted locations, recognizing that this represents the minimum distance traveled.

Prior to using the state-space models, we excluded 2 types of data. First, we excluded all locations within the species' breeding range (as defined by Tracy et al. 2020) up to July 4, the latest date red phalaropes have been documented to initiate nests in the North American Arctic (R. Lanctot & S. Saalfeld unpubl. data). Later dates were also excluded when individuals remained at their last presumed breeding site past July 4. Second, we excluded all locations from individuals when we suspected the tag fell off or the individual died as indicated by a lack of directional movement (i.e. a shotgun pattern of locations in one general location due to the inherent inaccuracy of PTT tags), usually accompanied by an inconsistent transmission rate (i.e. temporal gaps in locations longer than 1 d). We used the location prior to the lack of movement or when data were inconsistently received as the last known location of an individual. After filtering the data, we offset locations with the same date and time (e.g. when 2 location solutions were given for a transmission) for a given individual by 1 s to allow the inclusion of all locations into the model and removed outlier locations that indicated the bird had traveled >90 km h^{-1} from the previous location, reflecting an unrealistic movement (Duijns et al. 2019).

We used the state-space locations to describe general migration patterns for individuals during their southward migration. We defined locations as being onshore if they were associated with land (i.e. occurring on land or within waterbodies on land), nearshore if they were in the ocean but closer (within roughly a few km) to the coast, or pelagic if they were in the open ocean far from the coast. Given the relative error of the estimated state–space locations, we did not assign specific distances from the coast when distinguishing between nearshore and pelagic locations, but rather used these terms qualitatively. However, pelagic locations generally refer to locations several kilometers from the coast. General terms such as offshore and marine were used to describe locations not occurring on land but with no reference to distance from the coast.

2.3. Predicting activity states

To identify stopover areas, we first classified the 8 h predicted locations from the entire post-breeding period into 2 *a priori* defined activity states: (1) migrating state: where individuals were quickly transiting with few turns between locations indicative of nonstop, directional flights (hereafter migrating locations) and (2) stopover state: where individuals were moving slowly with many turns between locations indicative of individuals searching for prey or resting (hereafter stopover locations). We predicted the activity state for each location within this 'post-breeding model' by fitting a hidden Markov model using the package 'moveHMM' (Michelot et al. 2016) in R. In this model, activity states were assigned based on step lengths (i.e. distance traveled between points) and turning angles (i.e. change in direction of travel from prior movement) between consecutive 8 h locations using the gamma distribution (Michelot et al. 2016). As initial parameter values were required for model estimation, we verified that the model had identified the maximum-likelihood estimates of the parameters by refitting the model 50 times with random initial parameter values (Michelot & Langrock 2019). We used the Viterbi algorithm to estimate the most likely sequence of movement states to have generated the observations based on the fitted model (Michelot et al. 2016).

Next, we investigated whether the distance to the coast influenced the probability of a bird switching between or staying within an activity state by rerunning the above model with the explanatory variable 'distance to coast' (NASA Ocean Biology Processing Group and R. P. Stumpf 2012; accessed 17 December 2021), downloaded using the Env-DATA System (Dodge et al. 2013) on Movebank (movebank.org). We restricted this analysis to post-breeding locations within the Beringia region (i.e. Beaufort, Chukchi, and Bering seas; Fig. 1) for 2 reasons. First, few birds were tracked south of this region (78% of locations were from Beringia; Fig. 2). Second, once birds reached the pelagic areas in the Pacific Ocean, they were far from the coast compared to nearshore areas used by birds in Beringia. Thus, there was an inconsistent relationship between distance to coast and activity state transition probabilities. For this 'Beringia-only model', we did not investigate the effect of other oceanographic variables on activity state due to missing data for several locations and dates (see Figs. S1–S9 in the Supplement for degree of missing data; www.int-res.com/articles/suppl/m729p001_supp.pdf). We identified the best-supported model (either intercept-only model or model with distance to coast) as having the lowest Akaike's information criterion (AIC) value (Burnham & Anderson 2002). Locations were assigned final activity states using the post-breeding model for locations outside of Beringia and from the Beringia-only model for locations within Beringia.

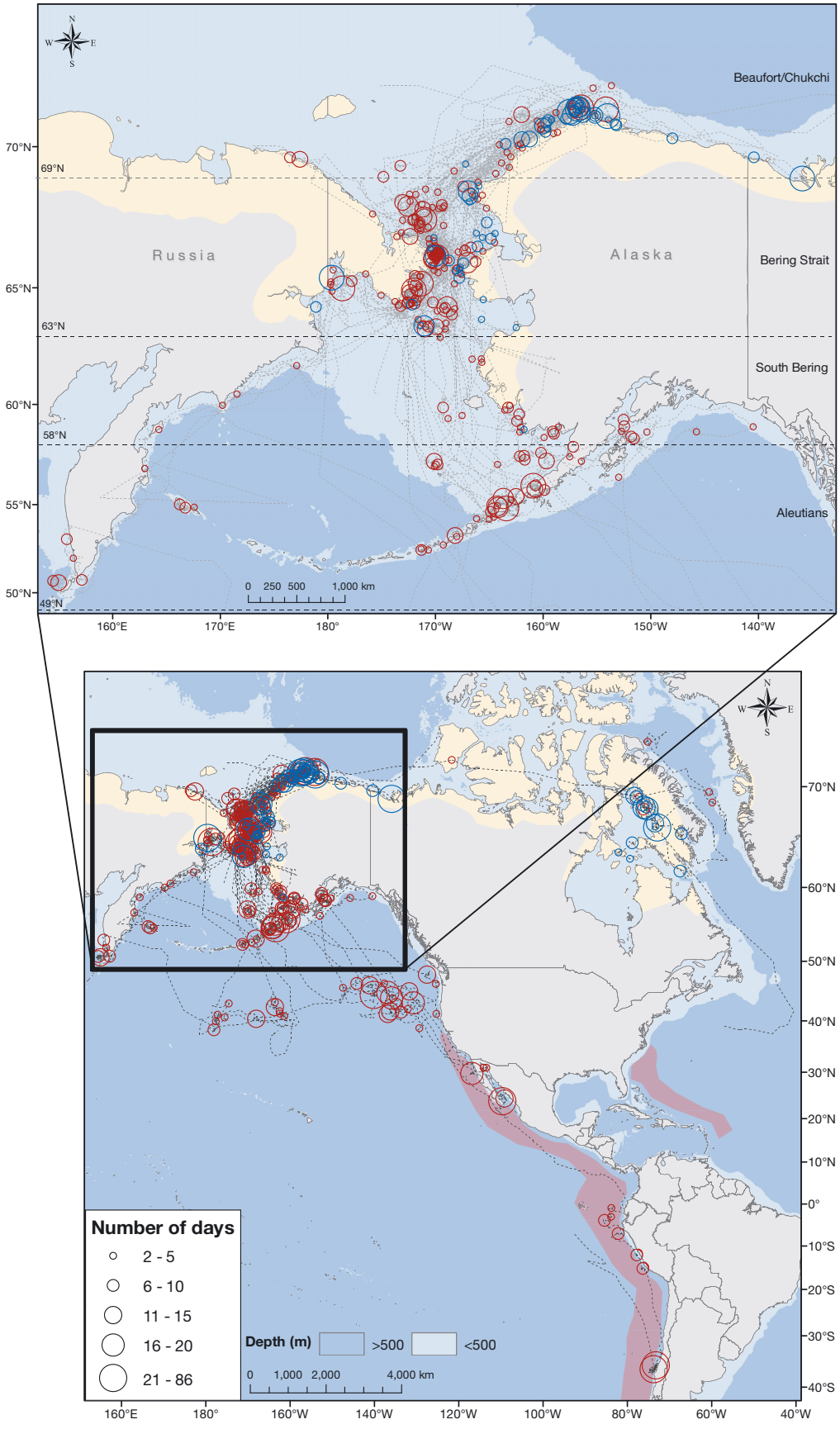

Fig. 2. Migration routes and stopover areas for female (red circles) and male (blue circles) red phalaropes during south and northward (one bird from Chile) migration (June–March) from 2017–2020; inset map illustrates the Beringia region in more detail. Predicted locations were generated every 8 h for individuals using continuous-time random walk state-space models; these locations were used to classify individual locations into a migrating or stopover activity state using hidden Markov models. Consecutive stopover locations were then combined to create stopover areas, depicted here as the mean center of all the points within a stopover area. Size of the legend symbol depicts the number of days an individual spent within a stopover area before migrating again. Note that starting locations for migration routes occur at the last site on the breeding grounds that was occupied on or before July 4. Red phalarope breeding (yellow shading) and wintering (pink shading) areas are from BirdLife International and Handbook of the Birds of the World (2021). Bathymetry (blue shading) from Becker et al. (2009)

2.4. Identifying individual stopover areas and population-level high-use areas

We identified stopover areas for each individual by clustering consecutive stopover locations and delineated the size using a minimum bounding polygon in ArcGIS 10.8.1 (Environmental Systems Research Institute, Redlands, CA). We then calculated the number of days an individual was at a stopover area by subtracting the latest date from the earliest date an individual was at each area. Note, we may not have identified all stopover areas given the temporal resolution of our data, and we did not take into account the error associated with predicted point locations when estimating stopover size. Further, our stopover areas may have included wintering areas for a few individuals that were successfully tracked to the south Pacific, as we did not distinguish between wintering and stopover areas in this analysis.

We identified population-level high-use areas (all months and years combined) within 4 regions of Beringia (1) Beaufort/Chukchi: north of 69° N, (2) Bering Strait: between 63 and 69° N, (3) South Bering: between 58 and 63° N, and (4) Aleutians: between 49 and 58° N (Fig. 1). As tags failed at different locations throughout Beringia (most stopped prior to 49° N), having defined regions allowed us to estimate region specific metrics by summarizing tracking data from subsets of individuals that had complete tracks within a region (as opposed to restricting analyses to individuals with complete tracks from breeding to wintering areas). Within each region, we estimated kernel utilization distributions of stopover locations for each individual that had a complete track through a region and >5 stopover locations (minimum required for modeling) using the 'adehabitatHR' package (Calenge 2006) in R with the smoothing parameter estimated by the default ad hoc method. Finally, to identify population-level high-use areas, we averaged kernel utilization distributions within each region by summing individual kernel utilization distributions and dividing by the total number of individuals with complete tracks within a region (including those with <5 stopover locations, as these individuals had the opportunity to stop within a region), using the Raster Calculator in ArcGIS 10.8.1.

2.5. Oceanographic conditions

To determine the relationship between red phalarope movements and sea ice conditions, we compiled the daily estimates of sea ice concentration (Spreen et al. 2008; obtained from www.seaice.uni-bremen.de) and the marginal ice zone (US National Ice Center 2020) (all data accessed 14 February 2022) from late June to early August within the Beaufort/Chukchi region during each year. The sea ice concentration index depicted the location of the pack ice, while the marginal ice zone identified areas of sparse or broken sea ice where sea ice concentrations varied between 10 and 80% intermixed with areas of open ocean (Strong & Rigor 2013, US National Ice Center 2020). Relationships between red phalarope movements and sea ice were then determined within 10 d periods from late June to early August each year by overlaying individual red phalarope migrating and stopover locations within each 10 d period on sea ice metrics based on the date in the middle of the 10 d period.

To better understand the oceanographic conditions present at red phalarope high-use areas within Beringia, we extracted satellite-derived, average monthly composites of sea surface temperature (JPL MUR MEaSUREs Project 2015, Chin et al. 2017; obtained from https://coastwatch.pfeg.noaa.gov/erddap, accessed 21 December 2021), sea surface salinity (Meissner et al. 2018, 2019; obtained from https://podaac-opendap.jpl.nasa.gov, accessed 19 December 2021), and chlorophyll *a* (chl *a*, an indicator of phytoplankton biomass reflecting the level of primary production; Hu et al. 2012, NASA Goddard Space Flight Center, Ocean Ecology Laboratory, Ocean Biology Processing Group 2018; obtained from https://coastwatch.pfeg.noaa.gov/erddap, accessed 8 December 2021), during each year of the study (2017–2020). As red phalarope high-use areas reflected population-level use primarily from July–September (<4% of all locations occurred in June and October) 2017–2020, we averaged monthly oceanographic variables from July–September across the same years to obtain average conditions during southward migration. We then qualitatively summarized the average oceanographic conditions within each high-use area. We did not consider annual or monthly relationships between red phalarope high-use areas and oceanographic conditions because low sample sizes of tracked red phalaropes, especially in 2019 and 2020, prevented meaningful analyses. However, we provide maps depicting monthly relationships between oceanographic conditions and stopover areas for each year in the Supplement (Figs. S1–S9).

2.6. Statistical analyses of movement metrics

For each individual, we estimated several tracking duration and migration metrics, including departure

date from breeding grounds, residency time, number of stopover areas, proportion of time at stopovers, and proportion of time on land. We calculated departure dates from the breeding grounds as the date an individual left its last breeding site (i.e. a site within the species' breeding range that was occupied on or before July 4). We estimated residency times within each Beringia region as the total number of 8 h locations for each individual regardless of activity state within a region divided by 3 (such that the unit of measure is the number of days). We calculated the proportion of time at stopovers and the proportion of time on land within Beringia regions as the number of stopover locations or locations on land (identified as having a distance to coast value $\leqslant 0$; see Section 2.3) for each individual within a region divided by the total number of locations within that region. We restricted calculations of residency time and the number of stopover areas to individuals with complete tracks for a given region. For calculations of the proportion of time at stopovers and the proportion of time on land, we used individuals with both complete and incomplete tracks for each region, as proportions account for the time individuals were within each region.

For each of these metrics, we then tested for assumptions of normality (Shapiro-Wilk test) and equal variances (Levene's test) using R. For variables that met these assumptions, we tested for differences within or between sexes, years, and/or Beringia regions (see Section 2.4) using an analysis of variance (ANOVA) in R; for variables that did not meet these assumptions, we used a Kruskal-Wallis test. Using similar methods, we also compared departure dates from the breeding grounds between males with successful and failed nests. Finally, we used a linear mixed effects model (with individuals included as a random effect) to compare dates females were present within each Beringia region between years using the package 'lme' (Bates et al. 2015) in R. In all analyses, we used an alpha level of 0.05 to indicate significance.

3. RESULTS

3.1. Tracking duration

Of the 103 red phalaropes tagged, 72 individuals (50 females, 22 males) transmitted during the post-breeding period, including 67 of 94 in Alaska and 5 of 9 in Canada (Table 1). Individuals were tracked for an average of 58 d (range: 5–275), with females transmitting, on average, 28 d longer than males (Kruskal-Wallis $\chi^2 = 7.34$; $p = 0.007$; Table 2). One female migrated over 33 000 km, which included travel to the wintering area and part of its return north. However, most individuals were tracked shorter distances, with the average individual traveling 5401 km (range: 206–33 364 km) before their tag stopped transmitting. Females, on average, were tracked >4000 km more than males (Table 2, Fig. 2). Three tagged females were known to have died prior to their departure from their breeding site at Utqiaġvik: one was killed by parasitic jaegers *Stercorarius parasiticus*, another was killed by a subsistence hunter, and a third was found with a broken wing after flying into a powerline.

3.2. Migration patterns in the Western Hemisphere

3.2.1. Departure date from the breeding grounds

Red phalaropes exhibited large individual variability in the start of post-breeding migration. In general, individuals left their last breeding site between late June and mid-August, with females, on average, leaving 17 d earlier than males (Kruskal-Wallis $\chi^2 = 36.92$; $p < 0.001$; Table 2, Fig. S10). Female departure dates varied by 33 d and males by 40 d. Some variability in female departure dates was explained by annual differences, with average departure being 7 d earlier in 2017 than in 2018 (Kruskal-Wallis $\chi^2 = 19.82$; $p < 0.001$; Table 2). Males tended to leave later in 2019 as compared to 2020, but the difference was not significant (ANOVA $F_{1,20} = 1.13$; $p = 0.30$; Table 2). Surprisingly, males with successful nests departed at similar dates (mean: 25 July; range: 11 July–14 August; n = 9) to males with unsuccessful nests (mean: 18 July; range = 5 July–13 August; n = 9; ANOVA $F_{1,16} = 1.40$; $p = 0.25$). We found similar results when analyses were restricted to males captured in Alaska.

3.2.2. Identification of activity states

Using location information in the Western Hemisphere, the post-breeding (intercept-only) model identified stopover locations as having a mean step length of 12.4 km (SD = 11.5 km) and a mean turning angle of −0.13° (concentration = 0.04), compared to migrating locations with a mean step length of 81.2 km (SD = 71.6 km) and mean turning angle of 0.02° (concentration = 1.39). The concentration measure indicates how clustered the turning angles are around the mean, with large values indicating directional movements and values close to zero indicating undirected movements (Michelot & Langrock 2019).

Table 2. Summary of migration and tracking information obtained during southward migration for female and male red phalaropes fitted with 2 g solar-powered Argos platform transmitter terminal (PTT) tags from 2017–2020. All data are restricted to locations and individuals tracked during post-breeding. All values are mean (range) unless otherwise stated. Last breeding site: a site within the species' breeding range occupied on or before July 4. Last breeding site may not have been the location the PTT tag was attached if the individual moved prior to July 4. Time between locations: time between successive locations obtained from PTT tags. Time = 0.0 corresponds to <3 min (0.05 h). No. of locations obtained: total no. of post-breeding locations obtained per individual from PTT tags. No. of days tracked: no. of days between the date an individual left its last breeding site and the date the last location was received or the date on which the tag was presumed to have fallen off or the individual died. Date of last location: date of the last location received or the date on which the tag was presumed to have fallen off or individual died. Distance tracked: distance traveled from when an individual left its last breeding site to the last transmission received or the date on which the tag was presumed to have fallen off or individual died. Distances were calculated as cumulative geodesic distances between predicted locations generated every 8 h for individuals using continuous-time random walk state-space models. **Bold** represents summaries by sex or location or across all individuals

Category	No. of individuals	Departure date from last breeding site	Time (h) between locations	No. of locations obtained	No. of days tracked	Date of last location	Distance (km) tracked
2017 (females, Alaska)	28	1 Jul (25 Jun–9 Jul)	2.4 (0.0–75.9)	708 (230–2490)	69 (13–275)	9 Sep (17 Jul–29 Mar)	6616 (1087–33 364)
2018 (females, Alaska)	22	8 Jul (2 Jul–28 Jul)	2.3 (0.0–84.9)	666 (24–1571)	63 (5–172)	9 Sep (12 Jul–27 Dec)	6970 (999–18 086)
2019 (males)	15	23 Jul (8 Jul–14 Aug)	1.3 (0.0–73.2)	724 (62–1742)	38 (7–89)	31 Aug (19 Jul–23 Oct)	2475 (288–9981)
Alaska-only	10	25 Jul (8 Jul–14 Aug)	1.2 (0.0–40.8)	813 (282–1742)	40 (13–89)	4 Sep (3 Aug–23 Oct)	2326 (457–5499)
Canada-only	5	20 Jul (11 Jul–1 Aug)	1.5 (0.0–73.2)	547 (62–1164)	35 (7–87)	23 Aug (19 Jul–10 Oct)	2773 (288–9981)
2020 (males, Alaska)	7	17 Jul (5 Jul–1 Aug)	1.0 (0.0–50.7)	922 (421–1919)	40 (18–89)	26 Aug (27 Jul–13 Oct)	1878 (206–5448)
Total (females)	**50**	**4 Jul (25 Jun–28 Jul)**	**2.3 (0.0–84.9)**	**689 (24–2490)**	**67 (5–275)**	**9 Sep (12 Jul–29 Mar)**	**6771 (999–33 364)**
Total (males)	**22**	**21 Jul (5 Jul–14 Aug)**	**1.2 (0.0–73.2)**	**787 (62–1919)**	**39 (7–89)**	**29 Aug (19 Jul–23 Oct)**	**2285 (206–9981)**
Alaska-only	**17**	**22 Jul (5 Jul–14 Aug)**	**1.1 (0.0–50.7)**	**858 (282–1919)**	**40 (13–89)**	**31 Aug (27 Jul–23 Oct)**	**2141 (206–5499)**
Canada-only	**5**	**20 Jul (11 Jul–1 Aug)**	**1.5 (0.0–73.2)**	**547 (62–1164)**	**35 (7–87)**	**23 Aug (19 Jul–10 Oct)**	**2773 (288–9981)**
Total (all individuals)	**72**	**9 Jul (25 Jun–14 Aug)**	**1.9 (0.0–84.9)**	**719 (24–2490)**	**58 (5–275)**	**5 Sep (12 Jul–29 Mar)**	**5401 (206–33 364)**

3.2.3. Identification of stopover areas

We identified 489 individual stopover areas (Fig. 2) that ranged in size from less than 1 to ~54 000 km^2 (mean = 1880 km^2). Stopover areas were occupied for less than 1 to up to 86 d (mean = 6 d; n = 489). The size of the stopover area generally increased with the time an individual remained at an area ($r = 0.64$; $p < 0.001$; Fig. 3B,C,D for example stopover areas).

3.2.4. Migration patterns and location of stopover areas in the Western Hemisphere

In general, red phalaropes tagged in Alaska migrated west into the Pacific Ocean while those tagged in the Central Canadian Arctic migrated east into the Atlantic Ocean (Fig. 2). However, 2 females and 1 male tagged in Alaska traveled east into Canada. Of those, 1 female and 1 male stopped on Banks Island and within the Mackenzie River Delta area, respectively, and then turned back to migrate toward Alaska. The other female continued to migrate across the Canadian Arctic, stopping at Banks Island for 2 d, then making numerous 1–6 d stops around Baffin and Prince Charles islands before the tag stopped transmitting (Fig. 2). Only 2 of the 5 individuals tracked during the post-breeding period in Canada provided locations away from the breeding grounds, stopping on and around Baffin and Prince Charles islands from late July to early October (Fig. 2). Only 1 individual provided locations farther south; this bird traveled non-stop (i.e. no stopover locations) for over 6 d, following the Labrador Current in early October, with its last transmission occurring in the Atlantic Ocean off the east coast of the United States on October 11 (Fig. 2).

Most of the 67 birds tagged in Alaska that provided post-breeding movements migrated west and then south through the Bering Strait before diverging to use either the Russian or Alaskan coastlines (Fig. 2; see Section 3.3 for more detailed information within Beringia). Three traveled (at least initially) eastward (see previous paragraph), and 11 stopped transmitting in the Beaufort/Chukchi region. Only 10 females were tracked south of the Bering Sea, where all stopped (often multiple times) within the North Pacific Current (38–46° N latitude and 129–179° W longitude; Fig. 2) between 1 and 24 d from late July to early January (Fig. 2). After spending ~27–107 d (mean = 49 d) within the

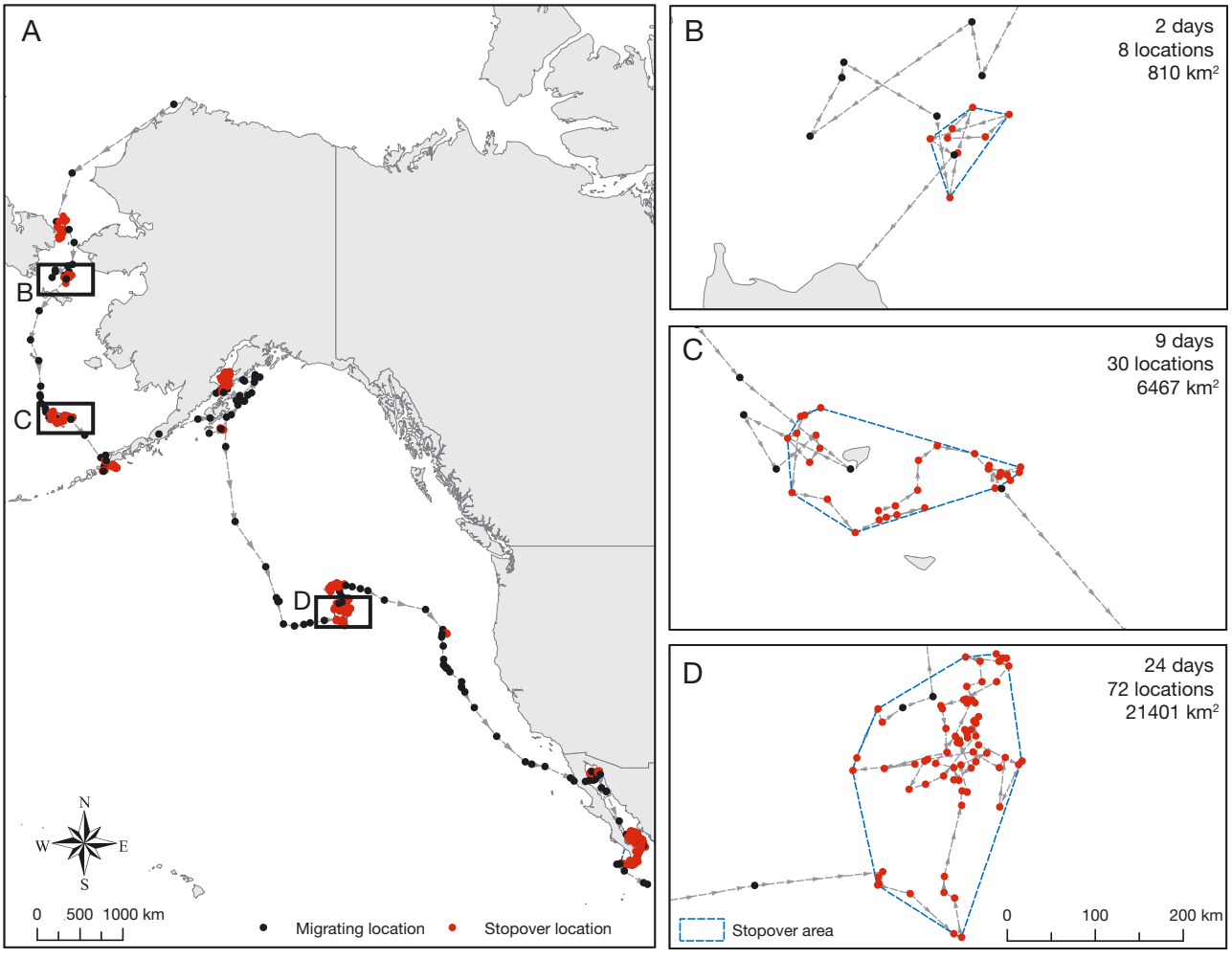

Fig. 3. Example (A) southward migration route and (B) small, (C) medium, and (D) large stopover areas for a female red phalarope tagged in Utqiaġvik, Alaska in 2018. Predicted locations were generated every 8 h using continuous-time random walk state-space models; these locations were used to classify locations as migrating or stopover using hidden Markov models. Stopover areas were delineated using a minimum bounding polygon around consecutive stopover locations

North Pacific Current, 5 individuals traveled southeast along the California Current, staying 0–527 km from the coast in both the Pacific Ocean and the Gulf of California (Fig. 2). Only 1 female was successfully tracked farther south, where it stopped at sites off the coast of Ecuador and Peru (Fig. 2), before traveling along the Humboldt Current to reach its wintering area off the coast of Chile in early December (Fig. 2). The southward migration distance for this female was 24 253 km. In its wintering area, it remained in a relatively small area (~24 500 km^2), about 44 km (range: 0–119 km) off the coast of Concepción, Chile (Fig. 2). On 25 March, it migrated north, staying farther from the coast (~300–1200 km) than during its southward migration; it was tracked >4000 km (~29° latitude) northwest before transmissions stopped (Fig. 2).

3.3. Migration patterns in Beringia

3.3.1. Identification of activity states

Within Beringia, the model including distance to coast as a covariate was a better supported model (AIC = 115 978; w_i = 1.0) than the intercept-only model (AIC = 116,085; w_i = 0.0) to predict activity states. Individuals closer to the coast were more likely to transition to and remain in a stopover state compared to individuals farther from the coast (Fig. 4). Stopover locations had a mean step length of 11.6 km (SD = 10.8 km) and a mean turning angle of 3.11° (concentration = 0.04), compared to migrating locations with a mean step length of 69.7 km (SD = 61.3 km) and a mean turning angle of 0.03° (concen-

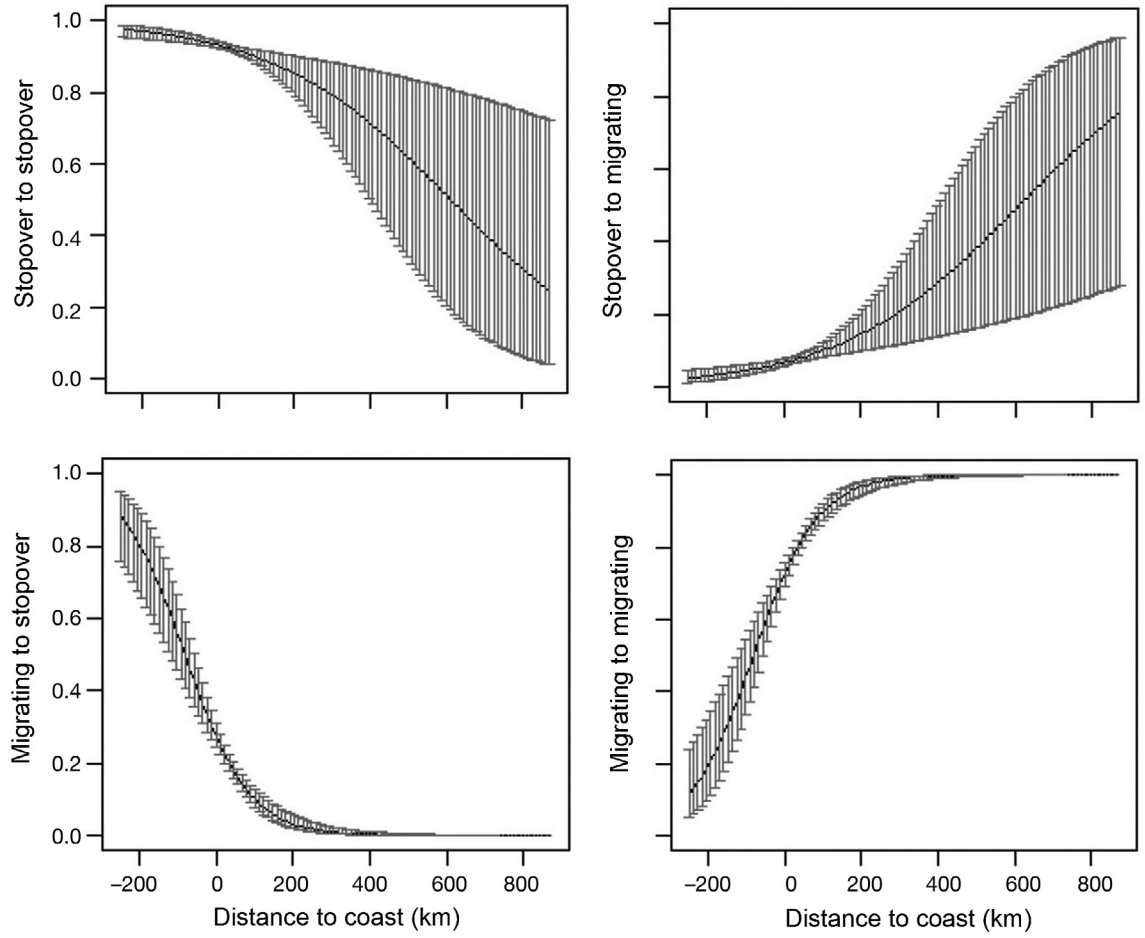

Fig. 4. Transition probabilities (i.e. the probability of switching states or remaining in the same state) as a function of distance to coast (negative distance values indicate birds were on land) with 95% confidence intervals for red phalaropes during southward migration in Beringia based on data from 2017–2020. Predicted locations were generated every 8 h for individuals using continuous-time random walk state-space models with migrating and stopover activity states classified by hidden Markov models

tration = 1.09). Stopover locations occurred in all 4 Beringia regions, with 56% of individuals with full tracks in a region stopping in the Beaufort/Chukchi, 100% in the Bering Strait, 42% in the South Bering, and 100% in the Aleutian region (Figs. 2 & S11).

3.3.2. Individual variability

Red phalaropes that migrated through the 4 Beringia regions showed large variability in movement behavior. While both males and females generally migrated southwest in the Beaufort/Chukchi seas, south in the Bering Strait and South Bering, and southeast in the Aleutians, movements in all directions also occurred, many over considerable distances (e.g. >200 km) in directions not consistent with the expected migration route (Fig. 5). Individuals meandered in all directions and even backtracked as they made their way through Beringia toward their wintering areas (see Fig. 3A for an example individual migration route and Fig. 2 for migration routes of all individuals). In contrast, while at stopover areas, males and females traveled mostly short distances (<25 km) in virtually all directions, although movements >25 km occurred occasionally, especially among females (Fig. 5). We also found considerable variability in when individuals migrated through each region, with individuals present in all regions as early as July and as late as October (Fig. 6).

3.3.3. Annual differences

Individual variability among females could generally not be attributed to a year effect, as the dates

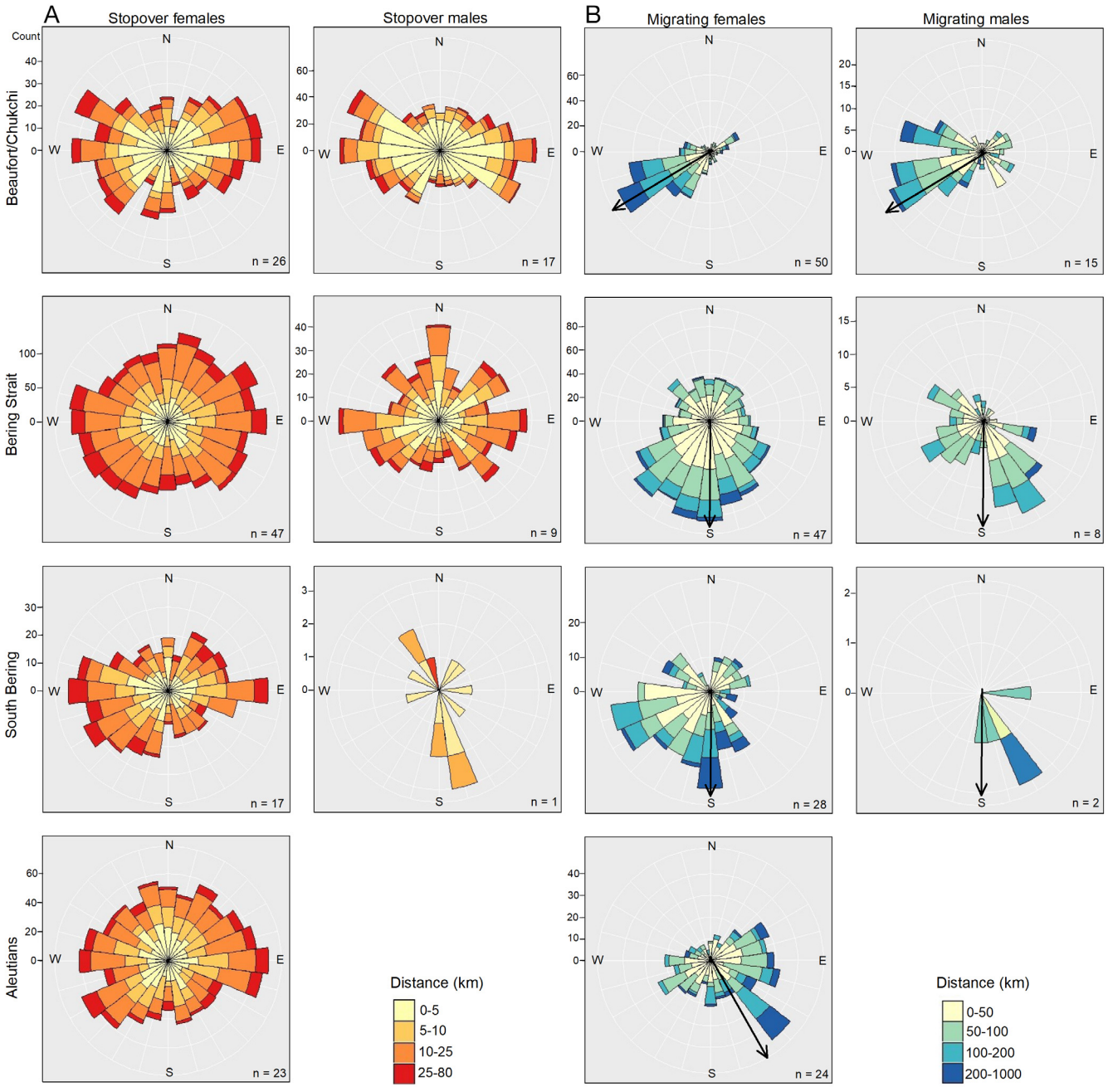

Fig. 5. Counts of directional movements within distance categories between consecutive locations for (A) stopover and (B) migrating male and female red phalaropes during southward migration through 4 regions in Beringia (see Fig. 2; data from 2017–2020; n = no. of individuals). No males were tracked into the Aleutian region. All data presented in this figure are based on predicted locations generated every 8 h for individuals using continuous-time random walk state-space models with stopover and migrating activity states classified by hidden Markov models. Directional bearings between consecutive locations calculated using the 'Argosfilter' package (Freitas 2013) in R (R Core Team 2021). Directional arrows illustrate the expected direction of migration through a region. Count legends are to the left of each figure but differ in their scales

present, the number of days present, the number of stopover areas, the proportion of time at stopovers, and the proportion of time on land within each region were similar for females in 2017 and 2018, suggesting a similarity in migration behavior between years. The only exception occurred in the Beaufort/Chukchi region where females were present later (linear mixed effects model $t_{1,48} = 2.06$; $p = 0.045$) and spent more time on land (Kruskal-Wallis $\chi^2 = 15.95$; $p < 0.001$) in 2018 (date present: mean = 1 August; range = 2 July–

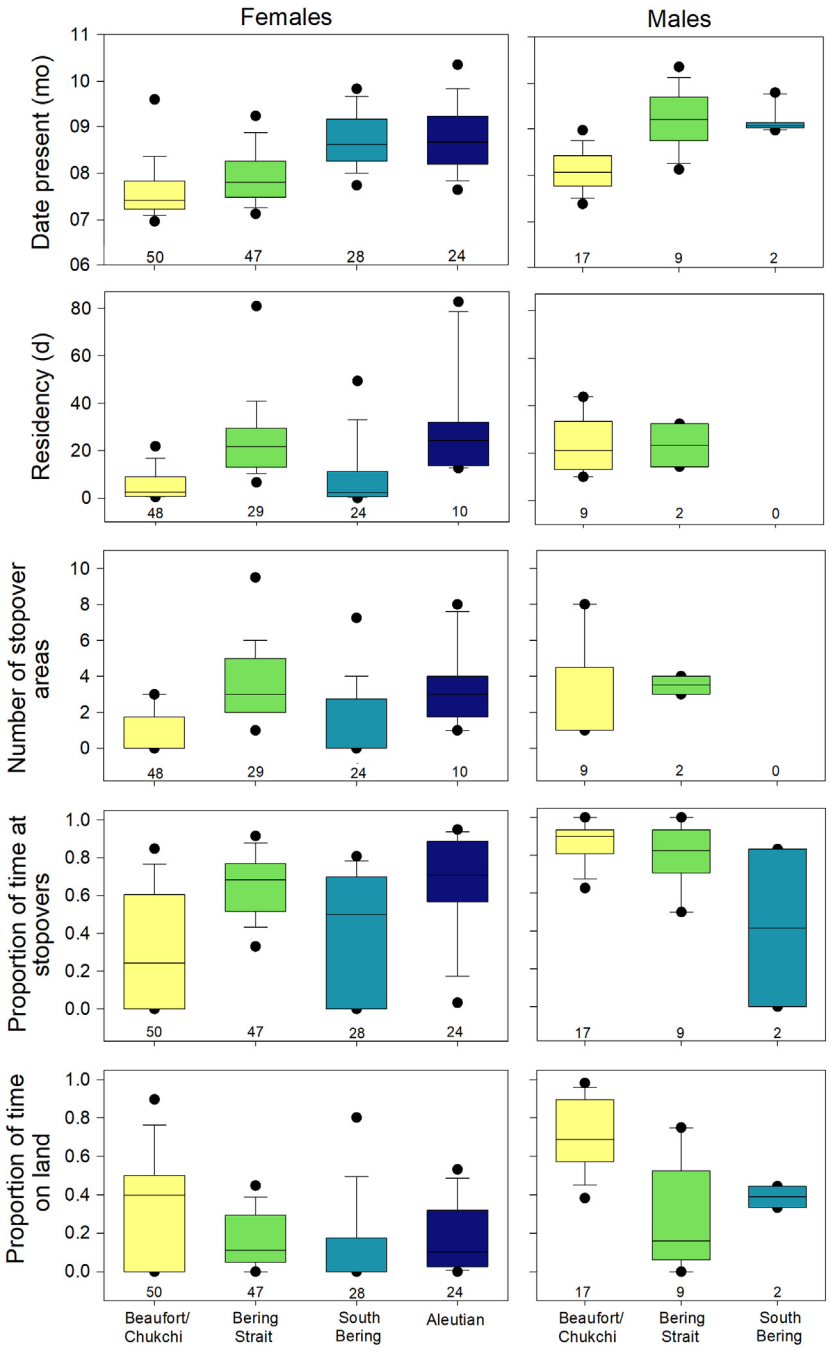

Fig. 6. Spatio–temporal patterns of male and female red phalarope presence during southward migration in 4 regions of Beringia (see Fig. 2; data from 2017–2020). Residency (in d) was calculated as the total number of 8 h locations regardless of state within a region divided by 3. Residency and number of stopover area calculations were restricted to individuals with complete tracks in a region, whereas date present, proportion of time at stopovers, and proportion of time on land were calculated from all individuals in a given region (sample sizes included at the bottom of each graph). No males were tracked into the Aleutian region. All data presented in this figure are based on predicted locations generated every 8 h for each individual using continuous-time random walk state-space models with stopover and migrating activity states classified by hidden Markov models. Boundaries of the box plots represent the 25th and 75th percentile, line within the box represents the median, error bars represent the 10th and 90th percentiles, and black dots represent the 5th and 95th percentiles

8 October; time on land: mean = 0.53; SE = 0.06; n = 22 ind.) compared to 2017 (date present: mean = 14 July; range = 25 June–14 August; time on land: mean = 0.19; SE = 0.04; n = 28 ind.). We were unable to conduct a similar analysis of annual differences in migratory behavior for males due to low sample sizes.

3.3.4. Sex differences

The Bering Strait and Aleutian regions were of great importance to female red phalaropes, as they spent more time (Kruskal-Wallis χ^2 = 50.20; $p < 0.001$), had more stops (Kruskal-Wallis χ^2 = 39.58; $p < 0.001$), and a higher proportion of time at stopovers (Kruskal-Wallis χ^2 = 35.20; $p < 0.001$) in these regions as compared to the Beaufort/Chukchi and South Bering regions (Fig. 6). Similar comparisons could not be made for males, as we had limited to no data within the South Bering and Aleutian regions; however, males also tended to have relatively longer residencies and numerous stops in the Beaufort/Chukchi and Bering Strait regions (Fig. 6). In the Beaufort/Chukchi region, post-breeding females (Kruskal-Wallis χ^2 = 15.68; $p = 0.001$) and males (ANOVA $F_{2,25}$ = 14.48; $p < 0.001$) spent a greater proportion of time on land compared to all other regions (Fig. 6). Compared to females, males spent more time within stopover areas in both the Beaufort/Chukchi (Kruskal-Wallis χ^2 = 31.26; $p < 0.001$) and Bering Strait (ANOVA $F_{1,54}$ = 6.78; $p = 0.012$; Fig. 6) regions. Post-breeding males also made more stops (Kruskal-Wallis χ^2 = 6.88; $p = 0.009$), stayed longer (Kruskal-Wallis χ^2 = 16.16; $p < 0.001$), and spent more time on land (Kruskal-Wallis χ^2 = 19.16; $p < 0.001$) in the Beaufort/Chukchi region than females (Fig. 6).

3.3.5. Identification of individual stopover areas and population-level high-use areas

Within Beringia, red phalarope individual stopover areas occurred both on land and at sea and were concentrated along the Alaska coastline of the Beaufort and Chukchi seas, along the Russian coastline of the Chukotka Peninsula, throughout the Bering Strait, and along the Aleutian Islands in Alaska, especially near Unimak Island (Fig. 2). Similar population-level high-use areas were found using kernel utilization distributions including the Alaska coastline of the Beaufort and Chukchi seas, along the Russian side of the Bering Strait, especially on the eastern and southern coastlines of the Chukotka Peninsula, around the Pribilof Islands in Alaska, and along the Alaskan Peninsula and Aleutian Islands, especially near Unimak Island in Alaska (Fig. 7).

3.3.6. Oceanographic conditions by region

Within the Beaufort/Chukchi region, red phalaropes were present from late June to mid-September, with most occurrences in July and August (Fig. 6). Many stopover locations occurred both onshore and in nearshore areas (Fig.2 & S11). This was the only region that had sea ice when red phalaropes were present, with high sea ice concentrations occurring throughout much of July in 2018 and 2020 but having retreated to the north by early July in 2017 and 2019 (Fig. 8). Occasionally, individuals migrated over areas with high sea ice concentration, but rarely stopped (Fig. 8). In contrast, females frequently foraged within the marginal ice zone, which is characterized by broken sea ice intermixed with open water, whereas males stayed on land or in open water (Fig. 8). Population-level high-use areas had relatively low average sea surface temperatures (<8°C; Fig. 9). Within the western portion of this region, higher average salinities (>30 PSU) occurred due to the northward-flowing currents through the Bering Strait (Fig. 9). Average chl *a* concentrations were relatively high (>3 mg m^{-3}) nearshore but declined farther from the coast (<1.5 mg m^{-3}; Fig. 9).

Within the Bering Strait region, red phalaropes were present from late June to October (Fig. 6), with most stopover locations occurring in pelagic areas, although a few locations were along both the Russian and Alaskan coastlines, as well as on St. Lawrence Island, Alaska (Figs. 2 & S11). Population-level high-use areas had relatively moderate average sea surface temperatures (6–10°C), high salinity (>30 PSU) likely due to the Anadyr Current (Fig. 9), and relatively high average chl *a* concentrations (many areas >4 mg m^{-3}; Fig. 9).

Within the South Bering region, red phalaropes were present from mid-July to October (Fig. 6) but had fewer stopover locations (relative to migrating locations) compared to all other regions (Figs. 2 & S11). Population-level high-use areas had relatively warm average sea surface temperatures (10–14°C) and low salinity (<30 PSU) likely due to the Alaskan Coastal Current (Fig. 9). Average chl *a* concentrations, however, were relatively high, especially along the Yukon-Kuskokwim Delta of Alaska (many areas >4 mg m^{-3}; Fig. 9). However, chl *a* concentration values, as estimated with satellite data, may be upward biased in nearshore areas, especially in areas with high turbidity from river inputs such as along the Alaska coastline (Chaves et al. 2015, Park et al. 2021).

Within the Aleutian region, red phalaropes were present from mid-July to October (Fig. 6), with many stopover locations occurring onshore and in nearshore areas, especially along the Alaska Peninsula and Aleutian Islands in Alaska (Figs. 2 & S11). Note, however, that data were available from only a few females this far south (Figs. 2 & S11). Population-level high-use areas were characterized by relatively high average sea surface temperatures (8–12°C), high salinity (>31 PSU), and low average chl *a* concentrations (i.e. most areas <2 mg m^{-3}, although patchy areas of high concentrations were present, especially near shore; Fig. 9).

4. DISCUSSION

Our study of post-breeding movements of red phalaropes from the North American Arctic suggests a relatively high level of migratory connectivity between breeding and wintering areas in the Atlantic and Pacific coast populations. As predicted, individuals generally took 2 distinct migration routes with most birds breeding in the Alaskan Arctic traveling toward the Pacific Ocean and birds breeding in the Central Canadian Arctic traveling toward the Atlantic Ocean. However, these 2 populations were not completely isolated, given that 2 females and 1 male that bred in Alaska travelled east, at least initially, into Canada. Taylor et al. (2011) also noted several red phalaropes making small-scale movements toward the east along the Alaskan coasts of the Chukchi and Beaufort seas, although the final migratory pathways of these individuals were undetermined. Similar deviations from expected migratory routes have been doc-

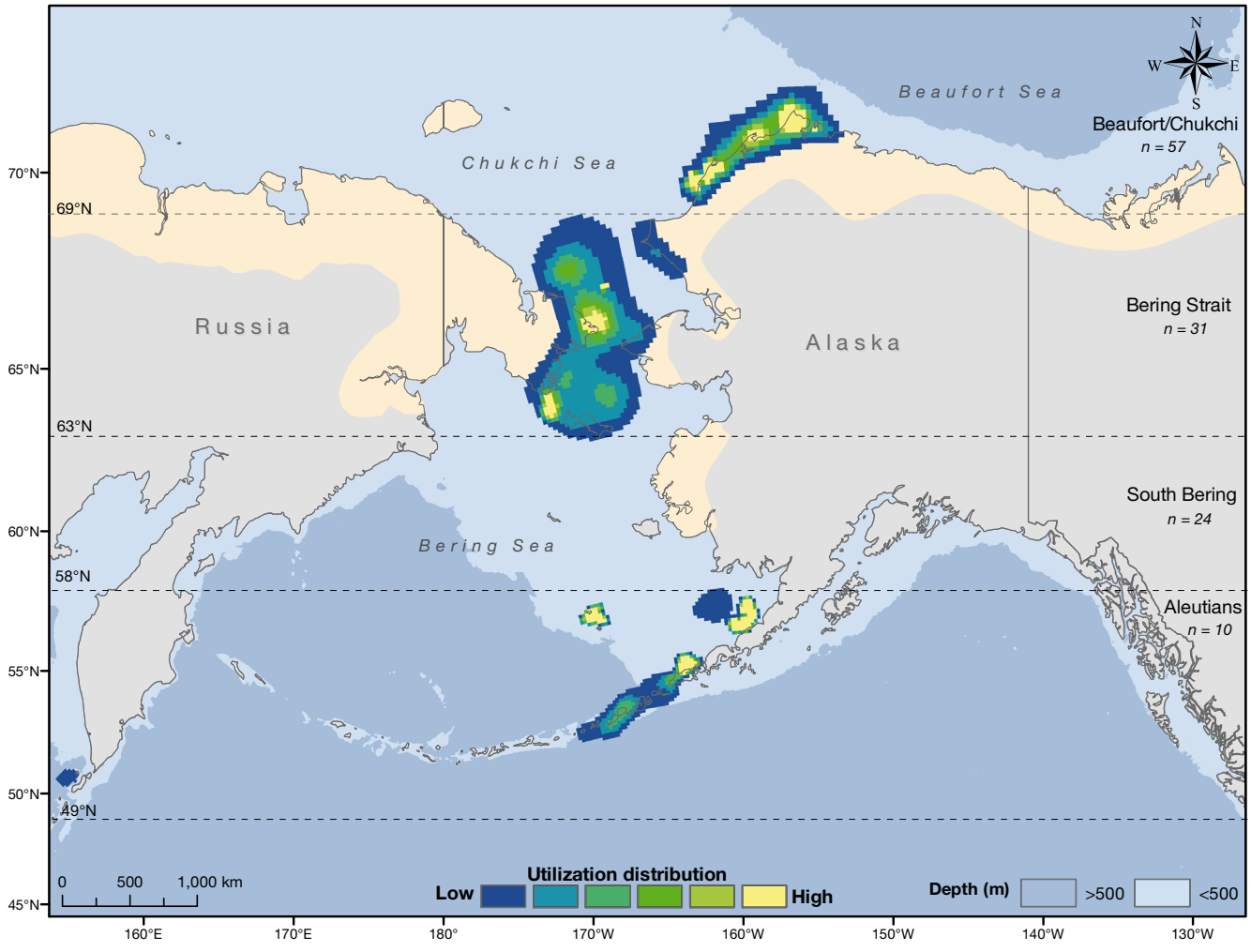

Fig. 7. Population-level high-use areas of red phalaropes during southward migration from June to October in Beringia from 2017–2020 (n = 48 females, 9 males). Kernel utilization distributions reflect the probability density of stopover locations averaged across individuals. Distributions were estimated within regions (indicated by dashed latitudinal lines; region names and sample sizes given on right side) using predicted locations for individuals with complete tracks through a region generated every 8 h using continuous-time random walk state-space models with stopover and migrating activity states classified by hidden Markov models. Red phalarope breeding (yellow shading) areas are from BirdLife International and Handbook of the Birds of the World (2021). Bathymetry (blue shading) from Becker et al. (2009)

umented for many seabirds, with such deviations often associated with a specific post-breeding dispersal stage (e.g. to molt; Cherel et al. 2016) or with searching for patchily distributed prey using olfactory cues (Nevitt 2008). A similar movement pattern was also noted for the short-tailed shearwater *Ardenna tenuirostris* using at-sea distributions in this same region, with individuals moving into the western Beaufort Sea before returning southwest toward southern breeding grounds (Kuletz et al. 2015, 2019). Thus, it is possible that foraging or other needs by seabirds within this region may necessitate short-term movements that do not follow their migratory routes.

4.1. Temporal and spatial variability in southward migration behavior

Red phalaropes varied in the timing, routes, and habitat selected during their southward migration. While females left Arctic-breeding sites about 2 wk earlier (on average) than males, both sexes left the breeding grounds over an extended period (females: 33 d; males: 40 d). The large variability in departure dates was not explained by year or by a male's breeding success; some individuals stayed at breeding sites well after the end of mating opportunities (females) or parental duties (males).

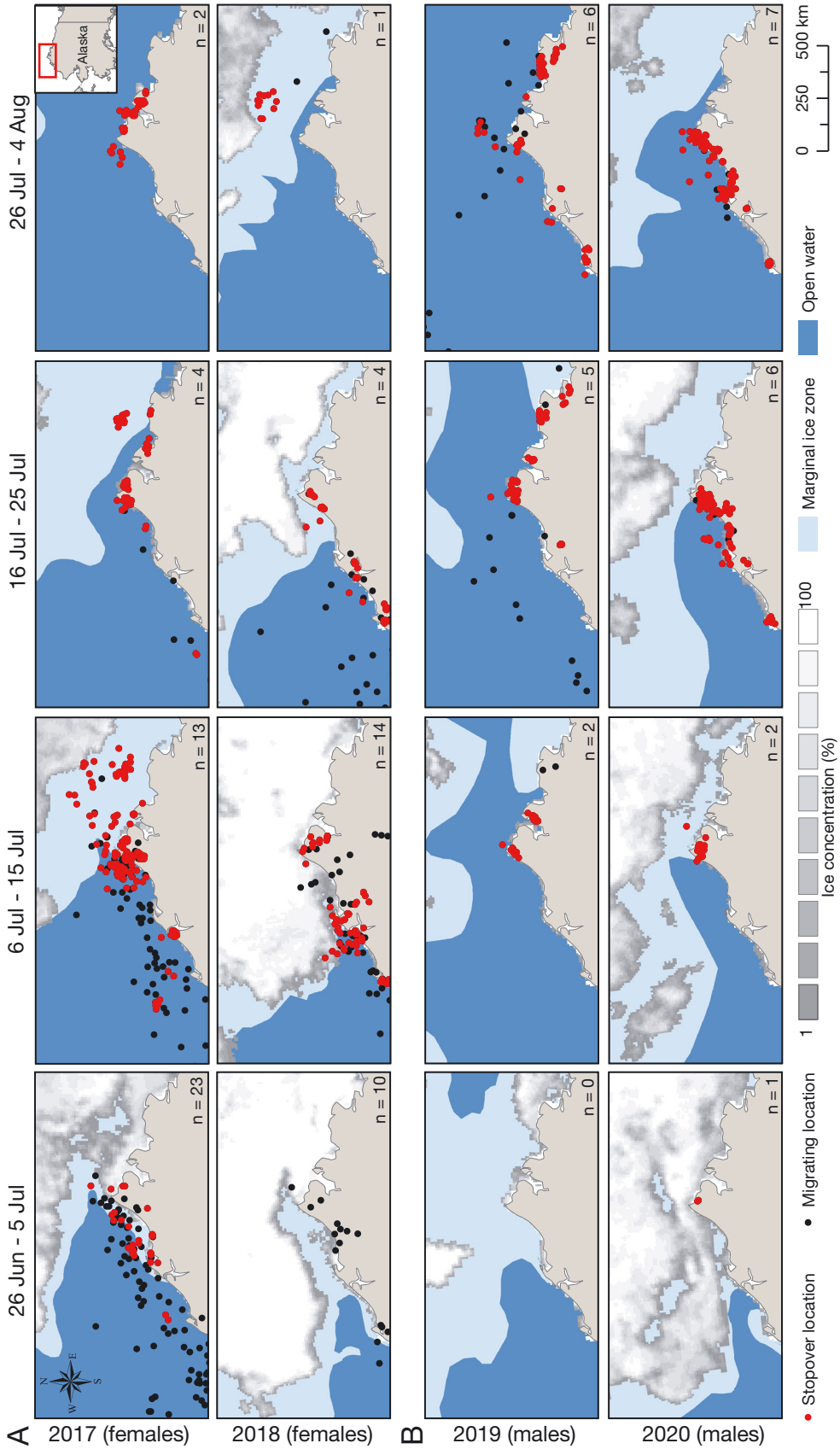

Fig. 8. Estimates of daily sea ice concentration (grey-scale) and marginal ice zone (light blue) from late June to early August 2017–2020 in relation to stopover and migrating locations of (A) female and (B) male red phalaropes in the Beaufort/Chukchi region. See Section 2.5 for definition of daily sea ice concentration and marginal ice zone. Activity states were classified based on hidden Markov models using predicted locations generated every 8 h from continuous-time random walk state-space models for individuals during southward migration. Panels include all red phalarope locations within each 10 d period, while estimates of daily sea ice concentration and the marginal ice zone reflect only a single date in the middle of the period (e.g. July 1 for the period 26 June–5 July). Number of individuals with displayed locations is shown on the bottom right of each panel

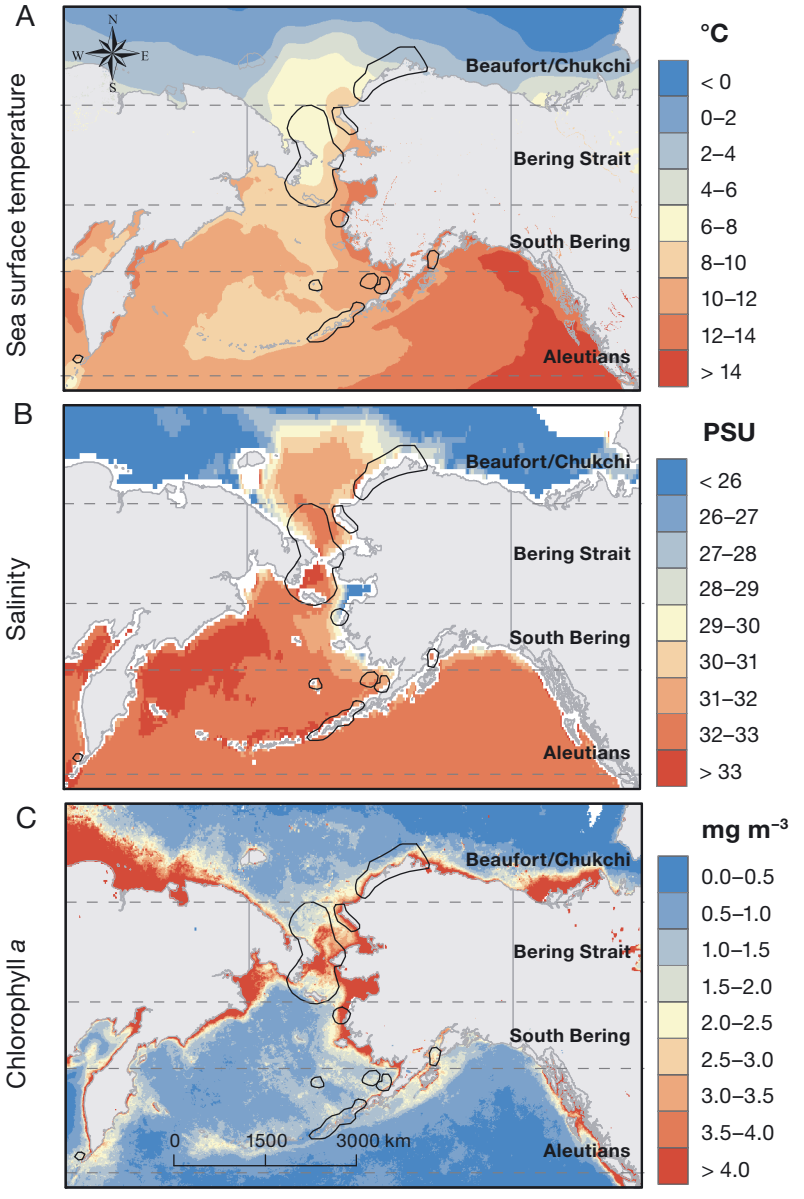

Fig. 9. Average (A) sea surface temperature, (B) salinity, and (C) chlorophyll *a* (chl *a*) concentrations from July–September 2017–2020 in relation to population-level high-use areas of red phalaropes (black outlined areas) within 4 regions (separated by dashed latitudinal lines with names on the right) in Beringia. Note that chl *a* values (mg m^{-3}) estimated with satellite data may be upwards biased in nearshore areas, especially in areas with high turbidity from river inputs such as along the Alaska coastline (Chaves et al. 2015, Park et al. 2021)

After leaving breeding sites, individual red phalaropes (especially males) commonly used onshore and nearshore areas near their breeding sites as post-breeding areas, instead of moving to the pelagic environment (Figs. 2 & 8). This was apparent at Utqiaġvik, Alaska, a previously identified important post-breeding site for red phalaropes (Connors et al. 1981, Smith & Connors 1993, Andres 1994, Taylor et al. 2010, 2011), where a prior study indicated post-breeding densities in nearshore habitats often exceeded breeding densities on the nearby tundra (Connors et al. 1979). Staging along the coast of the Beaufort/Chukchi region likely allows individuals to replenish energy reserves, especially males who have completed energetically expensive incubation and brood-rearing duties, prior to migrating to the pelagic environment. Indeed, a previous study noted red phalaropes feeding intensely on marine zooplankton along gravel beaches in this region (Connors et al. 1981). In addition, these post-breeding sites could be used by birds to molt, a process that begins during incubation (A. Taylor & R. Lanctot unpubl. data). Although onshore and nearshore areas in the Beaufort/Chukchi region appeared to be more important for males than for females, we cannot rule out that females used these areas as post-breeding sites prior to July 4 (the date we used to determine the start of post-breeding activities). This is because we were unable to determine whether females had completed breeding and females routinely moved large distances (>20 km) within the breeding area prior to July 4 (B. Kempenaers unpubl. data). Alternatively, the locations for acquiring energy or molting may differ between the sexes, with females, as the non-incubating sex, able to enter the pelagic environment sooner.

Individual red phalaropes exhibited tremendous variability in the route used to travel south toward their wintering areas, even when captured at the same breeding site. For example, individuals breeding in Utqiaġvik, Alaska, traveled west along the coasts of both Alaska and Russia, as well as east through the Canadian Arctic. van Bemmelen (2019) found similar spatial variability in red phalaropes migrating from Svalbard and Greenland through the Atlantic Ocean with individuals using 3 separate migration pathways and wintering areas. Furthermore, individuals migrating along common routes did not use the same stopover areas, although we did identify several population-level high-use

areas (often in highly productive areas) where multiple individuals stopped, presumably to forage (Fig. 7). Individuals also exhibited extreme deviations from a direct route to their wintering areas. Instead, individuals traveled in all directions, with much backtracking and meandering. For example, the 1 individual female tracked to its wintering area traveled ~9000 km (>35% of its >24000 km journey) more than a direct route would have necessitated (Fig. A1 in Appendix B). Such non-direct movements could indicate selective foraging in the dynamic pelagic environment where food resources are often patchy, ephemeral, or unpredictable in occurrence (Hyrenbach et al. 2000, Palacios et al. 2006, Weimerskirch 2007). Supporting this idea is the finding that phalaropes, unlike most other marine birds, have a higher variance in at-sea survey counts among years than among regions (Kuletz et al. 2019), suggesting phalaropes can respond to changes in prey availability more readily than other pelagic species. In addition to high spatial variability in migration patterns, red phalaropes also showed high temporal variation in their southward migration, with individuals present in all regions as early as July and as late as October. The few phalaropes we still tracked south of Beringia left between late July and late October (Fig. S10). This coincides with eBird (http://www.ebird.org; accessed 3 December 2023) observations showing greater weekly counts of red phalaropes off the coasts of Oregon and Washington, USA, throughout October and November.

While red phalaropes appear to use an obligate migration strategy when departing from the Arctic tundra (i.e. all individuals migrated south into the pelagic environment), the species' high spatial and temporal variability suggests they switch to a more facultative migration strategy once they enter the pelagic environment (Newton 2012). This is unlike most other long-distance, especially terrestrial, avian migrants that appear to be highly consistent in both the timing and path of their migration (i.e. traits of an obligate migration strategy), allowing individuals to take advantage of a limited number of stopover areas with highly predictable conditions as they make their way to the same wintering areas year after year (Newton 2012). In contrast, red phalaropes traveling in a highly ephemeral pelagic environment likely benefit from a more facultative migration strategy in which individuals migrate in response to food availability, stopping in areas where food is plentiful and moving when food supplies decline. This flexible migration behavior is consistent with the fly-and-forage migration patterns described in other seabirds (Amélineau et al. 2021), allowing individuals to respond to changes in resource availability.

The highly ephemeral pelagic environment may also prevent red phalaropes from having fixed, discrete wintering areas, but rather be reliant on vast areas to track variable food resources. While we were unable to track many red phalaropes into the wintering period, those we did track appeared to winter off the Pacific coast along a large latitudinal gradient, spanning from Washington, USA, to Chile (Fig. 2). However, cessation of tag transmissions prevented us from knowing whether some of these individuals eventually migrated farther south. Nonetheless, our results suggest that red phalaropes do not have a single discrete wintering area but rather use vast oceanic areas during the winter months. Similar results were found in the Atlantic population of red phalaropes, with individuals found continuously roaming across vast areas off the coast of the USA from roughly New Jersey to Virginia, blurring the transition between migration and wintering (van Bemmelen 2019). However, one individual in our study was observed wintering within a relatively small area of the Humboldt Current, suggesting that not all individuals follow this itinerant lifestyle during the wintering period. Similar results were also found in the Atlantic population of red phalaropes, in which several individuals were observed wintering in a relatively small area of the Canary Current (van Bemmelen 2019). Therefore, wintering in areas with stable conditions such as in highly productive ocean currents can likely support a more sedentary lifestyle during the wintering period (van Bemmelen 2019). The level of site-fidelity to specific wintering areas, however, remains unknown, as we have been unable to follow the same individuals for multiple years.

Given their reliance on finding ephemeral food resources during migration, migratory timing and movements of red phalaropes are likely to be greatly impacted by changes in oceanographic conditions, such as those caused by global climate change. For example, warmer waters, a longer open water season, and late plankton blooms may result in individuals staying longer in more northern areas, as has been shown by at-sea distributions for other migratory seabirds such as short-tailed shearwaters (Kuletz et al. 2020). Indeed, red phalaropes in this study were present in northern areas much later than expected, with individuals staying in the Beaufort/Chukchi region as late as October, and individuals wintering along the Pacific coast farther north than previously described (Tracy et al. 2020). Similar results found in red phalaropes along the Atlantic coast (van Bemmelen

2019) suggest that suitable foraging conditions may now be present farther north later in the season than they were historically.

4.2. Distributions in relation to oceanographic conditions

As with previous studies (Divoky 1979, Connors et al. 1981, Orr et al. 1982), we found that red phalaropes in the Beaufort and Chukchi seas, especially females earlier in the year, were often associated with the marginal ice zone (Fig. 8). Arctic sea ice is an important foraging habitat for many species, as it supports a community of ice-associated microalgae at the base of the food web (Gradinger 2009). These microalgae are foraged upon by a variety of zooplankton such as ice-associated amphipods (Hop et al. 2021), which, in turn, are consumed by higher trophic levels such as fish, seabirds, and whales, with up to 24% of fatty acid material in higher trophic levels being derived from ice algae (Budge et al. 2008). Thus, foraging in areas with broken sea ice and open water leads may allow red phalaropes to exploit these ice-associated prey. A previous study in the Beaufort Sea found that red phalaropes collected at the ice edge were foraging primarily on gammarid amphipods, including the ice-associated amphipod *Apherusa glacialis*, as well as mysids and euphausiids (Divoky 1984). Global climate change and the resulting loss of sea ice, however, is a major threat to this potentially important food resource (Budge et al. 2008, Macias-Fauria & Post 2018, Hop et al. 2021). Indeed, from the 1980s to the 2010s the abundance of ice-associated amphipods has declined in concordance with dramatic reductions in sea ice extent and thickness (Hop et al. 2021). As the Arctic Ocean is predicted to become predominately ice-free during the summer by the end of the twenty-first century (Johannessen et al. 2004, Zhang & Walsh 2006) or as early as 2040 (Holland et al. 2006, Wang & Overland 2009, Overland & Wang 2013), this potentially important foraging habitat may no longer be available to red phalaropes as they leave breeding areas to return to the marine environment.

In contrast, solid pack ice, especially shore-fast ice, appeared to reduce use or limit movements, with few individuals either landing on or migrating across these areas. Indeed, when shore-fast ice was present, red phalaropes often remained onshore (Fig. 8). However, the use of onshore or nearshore habitats was not limited to areas and times with solid pack ice, as individuals commonly used these habitats throughout Beringia. This was unexpected, as extensive at-sea surveys have rarely detected phalaropes close to shore (Briggs et al. 1984, Brown & Gaskin 1988, Tyler et al. 1993, Wahl et al. 1993). Such widespread use of onshore and nearshore habitats suggests that these areas may provide important foraging opportunities or refuges for individuals during migration, especially in areas or at times when pelagic environments are inhospitable (e.g. during storms) or have lower productivity (Drever et al. 2018).

As expected, red phalarope stopover areas were often in areas of greater food availability, such as highly productive ocean currents, ocean fronts, or upwellings (Orr et al. 1982, Briggs et al. 1984, Haney 1985, Brown & Gaskin 1988, Day 1992, Tyler et al. 1993, Wahl et al. 1993, DiGiacomo et al. 2002). For example, in the Beaufort and Chukchi seas, red phalaropes stopped above Barrow Canyon (Figs. 2 & 7), an area that extends from the Chukchi shelf into the western edge of the Beaufort Sea, where upwellings periodically result in high productivity (see areas of high chl *a* in Fig. 9), especially compared to surrounding areas (Pickart et al. 2013, Citta et al. 2015, Pisareva et al. 2019). Based on at-sea surveys, Barrow Canyon and Hannah Shoal to the west were significant marine hotspots for phalaropes and other marine birds during summer (Kuletz et al. 2015, 2019, Gall et al. 2022). Indeed, Divoky (1984) found that Barrow Canyon was the only place in the Beaufort Sea where red phalaropes occurred in large numbers, presumably because the remainder of the Beaufort Sea had low primary production and prey densities. The Beaufort and Chukchi seas were especially important for post-breeding males, as they spent more time and made more stops in this region. The additional time spent in this area by males may be due to them being in poorer body condition, a result of having to incubate and raise chicks independently, necessitating longer foraging periods in highly productive areas before migrating farther south.

The Bering Strait region is a known hotspot for marine birds, including red phalaropes, and mammals due to its high productivity and because it is the only corridor between the Arctic and the Bering Sea (Kuletz et al. 2015). Our tracking results confirmed the importance of this region for red phalaropes, with stopover areas occurring primarily along the Russian coastline (north of the Chukotka Peninsula south to St. Lawrence Island; Figs. 2 & 7) in association with the cold, highly saline, and nutrient-rich (Fig. 9) Anadyr Current that brings nutrients and zooplankton northward from the Bering Sea (Coachman et al. 1975, Sambrotto et al. 1984, Iken et al. 2010). In contrast, the Alaskan Coastal Current that parallels the

Alaskan coastline is relatively warm, low in salinity, and nutrient-poor (Fig. 9), as it is highly influenced by river output (Coachman et al. 1975, Sambrotto et al. 1984, Iken et al. 2010). The Anadyr Current also contains more large-bodied copepods (a primary food item for red phalaropes) in comparison to the Alaskan Coastal Current, where smaller copepods dominate (Piatt & Springer 2003, Eisner et al. 2013). As a result, higher densities of red phalaropes, as well as other planktivorous avian species, have been detected within the Anadyr Current compared to the Alaskan Coastal Current during at-sea surveys (Elphick & Hunt 1993, Kuletz et al. 2020). The use of highly productive areas such as the Anadyr Current was perhaps even more important during our study years, as 2017–2019 were characterized by an unprecedented marine heatwave with exceptionally high sea surface temperatures and low sea ice in the Bering Sea, changes that ultimately lead to numerous cascading impacts to the marine food web (Duffy-Anderson et al. 2019, Jones et al. 2023). As a result, the offshore foraging distribution of some seabird species appeared to concentrate in highly productive areas such as the Anadyr Current and Barrow Canyon (Kuletz et al. 2020). It has been proposed that the climatic changes that began in 2017 signal a regime shift, with future years forecasted to have an increased frequency of low sea ice events and consequently disruptions to the marine food web (Ballinger & Overland 2022). As such, the importance of highly productive areas to foraging seabirds is likely to increase in the future.

Within the south Bering Sea, population-level high-use areas tended to be concentrated around the Pribilof Islands, the Alaska Peninsula, and the Aleutian Islands in Alaska (Figs. 2 & 7). However, at-sea surveys have also indicated that red phalaropes may occur in high densities along the Bering Sea shelf that follows the Bering Slope Current from Russia to the Aleutian Islands in Alaska and the inner shelf of the Alaska coastline (Kuletz & Labunski 2017). While the Bering Sea shelf is known for its high productivity (Springer et al. 1996; Fig. 9), the inner shelf is located within the nutrient-poor Alaskan Coastal Current. However, persistent fronts along the inner shelf may provide greater accessibility to prey in this region, at least in some years (Schneider 1982, Hunt et al. 2014). Due to the relatively low productivity of the south Bering Sea (Fig. 9), the use of the Alaska Peninsula and Aleutian Islands in Alaska as stopover areas is likely of great importance to migrating red phalaropes, especially in areas such as Unimak and False passes, where primary productivity can be relatively high (particularly along the northern edge; Fig. 9) due to the Alaska Coastal Current flowing northward between the islands creating convergent tidal fronts (Ladd et al. 2005, Mordy et al. 2005).

4.3. Caveats and information needs

While the tracked phalaropes in this study provided locations that were not biased by human search effort (e.g. as is the case for at-sea surveys), it is important to note that individuals with PTT tags may behave differently than individuals without tags. We also cannot exclude that individuals were negatively affected by the tags or the harness (or both). Tags and the associated attachment material may reduce flight performance, reduce foraging efficiency, increase energy expenditure, increase predation rates, or compromise insulation (Thaxter et al. 2016, Seyer et al. 2021). The inability to appropriately thermoregulate may be especially important in the Arctic marine environment where poor insulation and damp feathers can quickly lead to hypothermia and death, especially for species that have no opportunity to dry themselves on land (Seyer et al. 2021). The relatively short duration that tags sent data suggests birds may have been compromised (Table 2), although, we cannot rule out the possibility that birds died from natural causes (e.g. due to low food availability in the warmer than normal years; Duffy-Anderson et al. 2019, Romano et al. 2020, Will et al. 2020, Jones et al. 2023), tags fell off or failed (e.g. due to prolonged saltwater exposure or solar panels becoming covered with feathers or salt), or to a combination of these factors. Variable tracking success with harnesses has also been found in other marine birds such as gulls and skuas (Sittler et al. 2011, Maftei et al. 2015, Thaxter et al. 2016, Seyer et al. 2021, Harrison et al. 2022) and may depend on the interaction between tag mass, harness type (leg-loop or back-pack style), and foraging mode. However, a comparison of the timing of southward migration between tagged individuals and eBird observations (www.ebird.org; accessed 3 December 2023) in Washington and Oregon, USA, indicated that tagged birds reached these areas at similar times as the observational data, suggesting that tags did not hamper individuals or result in delayed migration.

Nonetheless, this study provides important initial data on red phalarope movements in the Western Hemisphere. Movement data from additional birds and breeding populations could further improve our knowledge of migratory connectivity, as well as the

degree of spatial segregation between birds wintering along the Pacific and Atlantic oceans. In addition, movement data from other Arctic-breeding sites such as Russia are important to determine global migratory patterns and high-use areas. Given our limited sample size of males, more information on male migration patterns would also improve our understanding of the extent of annual variability and habitat use. And, as is common for most migratory birds, nothing is known about juvenile migration patterns. Fine-scale selection patterns of oceanographic conditions are also needed to determine the specific oceanographic conditions individuals select for foraging. Such information could be used to predict how future oceanographic changes may impact this species but was not available given the spatial resolution of the Argos tags we used. Miniaturization of GPS-accuracy tags and fine-scale imagery (both temporally and spatially) of oceanographic conditions could provide this information in the future. Finally, we still lack information for the spring migration period when high-use areas and migration routes may differ from those during fall migration. Given their small size, low site fidelity, and almost exclusive use of the marine environment, understanding the migratory movements of red phalaropes is challenging and requires innovative approaches and new technologies to follow this species throughout its annual cycle.

4.4. Conservation implications

In this study, we identified important areas within Beringia for red phalaropes including onshore and nearshore habitats of the Beaufort and Chukchi seas, the western edge of the Bering Strait, along the Alaska Peninsula and Aleutian Islands, and the Pribilof Islands, Alaska (Fig. 7). These results complement studies by Kuletz et al. (2015), who identified important marine areas for red phalaropes in the Chukchi and Beaufort seas (including areas within and north of the Bering Strait, within Hope Basin, and several areas offshore between Cape Lisburne and Wainwright, Alaska) and Smith et al. (2014), who identified 4 globally important (i.e. containing ⩾1% of the global population) areas for red phalaropes within this region (2 in the Beaufort/Chukchi region, 1 between Seguam and Amlia islands along the Aleutian Islands, and 1 on the Bering Sea shelf). However, these areas do not account for foraging requirements throughout the species' entire migratory route given the ephemeral nature of the marine environment leading to seasonal and annual changes in the resources used by red phalaropes (Hyrenbach et al. 2000, Palacios et al. 2006).

While identification of important areas for marine species such as red phalaropes can be important for future conservation and management decisions (e.g. Hays et al. 2019, Davies et al. 2021), many threats to marine species are not site-specific. Global climate change caused by anthropogenic fossil fuel emissions is perhaps the greatest threat to marine ecosystems as warmer ocean temperatures and acidification are likely to result in a cascade of wide-spread impacts. For example, warmer temperatures and earlier sea ice retreat can change both the timing and magnitude of spring phytoplankton and zooplankton blooms (Hunt et al. 2002, Overland & Stabeno 2004, Arrigo et al. 2008, Sigler et al. 2016, Duffy-Anderson et al. 2019, Huntington et al. 2020), potentially resulting in a phenological mismatch or lower food availability for migrating red phalaropes (although, note that the opposite [i.e. an improved match] could also occur). Additionally, the composition of prey items such as zooplankton has shifted with warming temperatures. In the Arctic, zooplankton species have shifted from large- to small-bodied species in warmer years and their distribution shifted northward (Coyle et al. 2008, Hunt et al. 2011, Eisner et al. 2014, Duffy-Anderson et al. 2019), which may make high-value prey less available to migrating phalaropes. Along with changes in prey communities, predator communities are also changing. For example, the northward expansion of several fish species occurred with warmer temperatures (Hunt et al. 2002, Overland & Stabeno 2004, Grebmeier et al. 2006, Stevenson & Lauth 2019, Huntington et al. 2020, Mueter et al. 2021, Levine et al. 2023) and may result in added predation pressure on the zooplankton communities used by red phalaropes. Other species such as bowhead *Balaena mysticetus*, gray *Eschrichtius robustus*, and humpback whales *Megaptera novaeangliae* are also shifting their movements farther north and remaining there for longer periods of time (Moore et al. 2003, Moore 2016, Tsujii et al. 2021, Stafford et al. 2022). Given the potential benefits phalaropes obtain by symbiotically foraging near whales (Kumlien 1879, Nelson 1883, Harrison 1979, Obst & Hunt 1990, Day 1992, Grebmeier & Harrison 1992, Elphick & Hunt 1993), changes in the encounter rate between whales and phalaropes has the potential to impact phalarope populations. Climate change is also impacting habitat outside the pelagic environment. For example, many tundra areas are experiencing widespread surface water declines as a result of permafrost thaw (Webb et al. 2022), potentially impacting many species such as

red phalaropes that rely on wet tundra for nesting (Saalfeld et al. 2013, Cunningham et al. 2016). The degree to which climate-induced ecosystem changes will ultimately impact red phalarope populations remains unknown, but recent evidence suggests a negative impact, as phalarope populations have declined with warming temperatures and earlier sea ice retreat in the eastern Chukchi Sea (Gall et al. 2017).

Other anthropogenic impacts such as oil and gas exploration, vessel traffic, and wind farm development are also increasing at sea, potentially resulting in direct and indirect mortality of marine birds (Tyler et al. 1993, Wahl et al. 1993, Humphries & Huettmann 2014, Silber et al. 2021, Berkman et al. 2022). While the relative risk of these threats to red phalaropes are not well known, previous work suggests that these threats are likely not negligible. For example, both red and red-necked *Phalaropus lobatus* phalaropes have been found dead at coastal and offshore industrial sites in Atlantic Canada (Gjerdrum et al. 2021), presumably due to disorientation from artificial light. Moreover, red-necked phalaropes have been classified as moderately at risk of mortality due to collision at offshore wind turbines in England (Bradbury et al. 2014). Thus, current distributions and migration pathways of marine birds should be considered before any future developments associated with these activities occur. Perhaps of greatest importance are hotspots where numerous individuals stop to forage at the same time (e.g. large rafts of phalaropes observed in the Bering Sea; Gill & Handel 1981, Winker et al. 2002). Such aggregations can expose many individuals to risk should a localized disturbance (e.g. ship passing through) or pollution (e.g. oil spill) event occur. Marine birds are also at risk from the ingestion of plastics. Red phalaropes, as surface feeders, appear to be especially vulnerable to plastic ingestion (Moser & Lee 1992, Drever et al. 2018, Baak et al. 2020, Flemming et al. 2022), perhaps due to the species' preferential selection of oceanographic features that concentrate plastics such as convergences and eddies (Moore et al. 2001). For example, in our study, we showed that red phalaropes often stopped within the North Pacific Current, which is at the northern boundary of the plastic-laden 'Great Pacific Garbage Patch' (Lebreton et al. 2018).

While we learned a great deal about the southward migration of red phalaropes in the Western Hemisphere, many unknowns remain, including the impact of climate change and other anthropogenic impacts on the population. How the species fares will depend not only on the continued trajectories of climate change and other anthropogenic impacts, but also on the species' adaptability. The large variability in migration timing and routes observed in this study suggests that red phalaropes may be at least partially capable of adapting to changing conditions during the critically important migration stage, to what degree, however, remains unknown.

Acknowledgements. We thank the following field assistants for help tagging red phalaropes: Utqiaġvik (US Fish and Wildlife Service): Peter Detwiler, Lindall Kidd, Lindsay Hermanns, Kayla Scheimreif, Samuel Stone, and Daniel Catlin; Qupałuk: Peter Detwiler; Utqiaġvik (Max Planck Institute for Biological Intelligence): Margherita Cragnolini, Pietro D'Amelio, Martin Bulla, Peter Santema, Carol Gilsenan, Giulia Bambini, Kim Teltscher, Kristina Beck and Luisana Carballo; Cambridge Bay: Emma Sutherland, Kim Régimbald-Bélanger, Mia Courville-Todorov; East Bay: Ariel Lenske and Sarah Neima; and Igloolik: Marianne Gousy-Leblanc, Mathieu Archambault, Cléa Frapin, Mike Qrunuk, and Tommy O'Neil Sanger. Funding was obtained from the Max Planck Institute for Biological Intelligence, US Fish and Wildlife Service, Environment and Climate Change Canada, Bureau of Ocean Energy Management, the National Fish and Wildlife Foundation, ConocoPhillips Charitable Investments Global Signature Program in support of the Migratory Connectivity Project, Wilburforce Foundation, and Bureau of Land Management. We thank the Barrow Arctic Science Consortium and Umiaq LLC for logistic support in Utqiaġvik, and ConocoPhillips Alaska for logistical and in-kind support on the Colville River Delta. The Ukpeaġvik Inupiat Corporation and the North Slope Borough kindly permitted us to conduct this research on their lands. Any use of trade, product, or firm names is for descriptive purposes only and does not imply endorsement by the US Government. The findings and conclusions in this article are those of the author(s) and do not necessarily represent the views of the US Fish and Wildlife Service.

LITERATURE CITED

Alaska Shorebird Group (2019) Alaska shorebird conservation plan. Version III. Alaska Shorebird Group, Anchorage, AK

Amélineau F, Merkel B, Tarroux A, Descamps S and others (2021) Six pelagic seabird species of the North Atlantic engage in a fly-and-forage strategy during their migratory movements. Mar Ecol Prog Ser 676:127–144

Andres BA (1994) Coastal zone use by postbreeding shorebirds in northern Alaska. J Wildl Manag 58:206–213

Arrigo KR, van Dijken G, Pabi S (2008) Impact of a shrinking Arctic ice cover on marine primary production. Geophys Res Lett 35:L19603

Baak JE, Linnebjerg JF, Barry T, Gavrilo MV, Mallory ML, Price C, Provencher JF (2020) Plastic ingestion by seabirds in the circumpolar Arctic: a review. Environ Rev 28: 506–516

Ballinger TJ, Overland JE (2022) The Alaskan Arctic regime shift since 2017: a harbinger of years to come? Polar Sci 32:100841

Bates D, Mächler M, Bolker B, Walker S (2015) Fitting linear mixed-effects models using lme4. J Stat Softw 67:1–48

Becker JJ, Sandwell DT, Smith WHF, Braud J and others (2009) Global bathymetry and elevation data at 30 arc seconds resolution: SRTM30_PLUS. Mar Geod 32:355–371

Berkman PA, Fiske GJ, Lorenzini D, Young OR and others (2022) Satellite record of Pan-Arctic maritime ship traffic. In: Druckenmiller ML, Thoman RL, Moon TA (eds) Arctic Report Card 2022. NOAA Tech Rep OAR ARC 22-10. https://doi.org/10.25923/mhrv-gr76

BirdLife International and Handbook of the Birds of the World (2021) Bird species distribution maps of the world. Version 2021.1. http://datazone.birdlife.org/species/requestdis

Both C, Van Turnhout CAM, Bijlsma RG, Siepel H, Van Strien AJ, Foppen RPB (2010) Avian population consequences of climate change are most severe for long-distance migrants in seasonal habitats. Proc R Soc B 277: 1259–1266

Bradbury G, Trinder M, Furness B, Banks AN, Caldow RWG, Hume D (2014) Mapping seabird sensitivity to offshore wind farms. PLOS ONE 9:e106366

Briggs KT, Dettman KF, Lewis DB, Tyler WB (1984) Phalarope feeding in relation to autumn upwelling off California. In: Nettleship DN, Sanger GA, Springer PF (eds) Marine birds: their feeding ecology and commercial fisheries relationships. Canadian Wildlife Service, Environment Canada, Ottawa, p 51–62

Brown RGB, Gaskin DE (1988) The pelagic ecology of the grey and red-necked phalaropes *Phalaropus fulicarius* and *P. lobatus* in the Bay of Fundy, eastern Canada. Ibis 130:234–250

Budge SM, Wooller MJ, Springer AM, Iverson SJ, McRoy CP, Divoky GJ (2008) Tracing carbon flow in an arctic marine food web using fatty acid-stable isotope analysis. Oecologia 157:117–129

Burnham KP, Anderson DR (2002) Model selection and multimodel inference: a practical information-theoretic approach, 2nd edn. Springer, New York, NY

CAFF (2017) State of the Arctic marine biodiversity report. Conservation of Arctic Flora and Fauna International Secretariat, Akureyri

Calenge C (2006) The package 'adehabitat' for the R software: a tool for the analysis of space and habitat use by animals. Ecol Modell 197:516–519

Callaghan TV, Bjorn LO, Chernov YI, Chapin T and others (2005) Arctic tundra and polar desert ecosystems. In: Symon C, Arris L, Heal B (eds) Arctic climate impact assessment. Cambridge University Press, Cambridge, p 243–352

Chan YC, Brugge M, Tibbitts TL, Dekinga A, Porter R, Klaassen RHG, Piersma T (2016) Testing an attachment method for solar-powered tracking devices on a long-distance migrating shorebird. J Ornithol 157:277–287

Chaves JE, Werdell PJ, Proctor CW, Neeley AR, Freeman SA, Thomas CS, Hooker SB (2015) Assessment of ocean color data records from MODIS-Aqua in the western Arctic Ocean. Deep Sea Res II 118:32–43

Cherel Y, Quillfeldt P, Delord K, Weimerskirch H (2016) Combination of at-sea activity, geolocation and feather stable isotopes documents where and when seabirds molt. Front Ecol Evol 4:3

Chin TM, Vazquez-Cuervo J, Armstrong EM (2017) A multi-scale high-resolution analysis of global sea surface temperature. Remote Sens Environ 200:154–169

Citta JJ, Quakenbush LT, Okkonen SR, Druckenmiller ML and others (2015) Ecological characteristics of core-use areas used by Bering–Chukchi–Beaufort (BCB) bowhead whales, 2006–2012. Prog Oceanogr 136:201–222

Coachman LK, Aagaard K, Tripp RB (1975) Bering Strait: the regional physical oceanography. University of Washington Press, Seattle, WA

Connors PG, Myers JP, Pitelka FA (1979) Seasonal habitat use by arctic Alaskan shorebirds. Stud Avian Biol 2:101–111

Connors PG, Connors CS, Smith KG (1981) Shorebird littoral zone ecology of the Alaskan Beaufort coast. OCSEAP Final Report of Principal Investigators 23:297–396

Coyle KO, Pinchuk AI, Eisner LB, Napp JM (2008) Zooplankton species composition, abundance and biomass on the eastern Bering Sea shelf during summer: the potential role of water-column stability and nutrients in structuring the zooplankton community. Deep Sea Res II 55:1775–1791

Cunningham JA, Kesler DC, Lanctot RB (2016) Habitat and social factors influence nest-site selection in Arctic-breeding shorebirds. Auk 133:364–377

Cusset F, Fort J, Mallory M, Braune B, Massicotte P, Massé G (2019) Arctic seabirds and shrinking sea ice: egg analyses reveal the importance of ice-derived resources. Sci Rep 9:15405

Davies TE, Carneiro APB, Tarzia M, Wakefield E and others (2021) Multispecies tracking reveals a major seabird hotspot in the North Atlantic. Conserv Lett 14:e12824

Day RH (1992) Seabirds at sea in relation to oceanography. PhD dissertation, University of Alaska, Fairbanks, AK

Dierschke V, Furness RW, Garthe S (2016) Seabirds and offshore wind farms in European waters: avoidance and attraction. Biol Conserv 202:59–68

DiGiacomo PM, Hamner WM, Hamner PP, Caldeira RMA (2002) Phalaropes feeding at a coastal front in Santa Monica Bay, California. J Mar Syst 37:199–212

Divoky GJ (1979) Sea ice as a factor in seabird distribution and ecology in the Beaufort, Chukchi, and Bering seas. In: Bartonek JC, Nettleship DN (eds) Conservation of marine birds of northern North America. Wildlife Research Report 11. US Fish and Wildlife Service, US Department of the Interior, Washington, DC, p 9–17

Divoky GJ (1984) The pelagic and nearshore birds of the Alaskan Beaufort Sea: biomass and trophics. In: Barnes PW, Schell DM, Reimnitz E (eds) The Alaskan Beaufort Sea: ecosystems and environments. Academic Press, Orlando, FL, p 417–437

Dodge S, Bohrer G, Weinzierl R, Davidson SC and others (2013) The environmental-data automated track annotation (Env-DATA) system: linking animal tracks with environmental data. Mov Ecol 1:3

Douglas DC, Weinzierl R, Davidson SC, Kays R, Wikelski M, Bohrer G (2012) Moderating Argos location errors in animal tracking data. Methods Ecol Evol 3:999–1007

Drever MC, Provencher JF, O'Hara PD, Wilson L, Bowes V, Bergman CM (2018) Are ocean conditions and plastic debris resulting in a 'double whammy' for marine birds? Mar Pollut Bull 133:684–692

Duffy-Anderson JT, Stabeno P, Andrews AG III, Cieciel K and others (2019) Responses of the northern Bering Sea and southeastern Bering Sea pelagic ecosystems following record-breaking low winter sea ice. Geophys Res Lett 46:9833–9842

Duijns S, Anderson AM, Aubry Y, Dey A and others (2019) Long-distance migratory shorebirds travel faster towards their breeding grounds, but fly faster post-breeding. Sci Rep 9:9420

Eisner L, Hillgruber N, Martinson E, Maselko J (2013) Pelagic fish and zooplankton species assemblages in relation to water mass characteristics in the northern Bering and southeast Chukchi seas. Polar Biol 36:87–113

Eisner LB, Napp JM, Mier KL, Pinchuk AI, Andrews AG III

(2014) Climate-mediated changes in zooplankton community structure for the eastern Bering Sea. Deep Sea Res II 109:157–171

Elphick CS, Hunt GL Jr (1993) Variations in the distributions of marine birds with water mass in the northern Bering Sea. Condor 95:33–44

Flemming SA, Lanctot RB, Price C, Mallory ML and others (2022) Shorebirds ingest plastics too: what we know, what we do not know, and what we should do next. Environ Rev 30:537–551

Freitas C (2013) Package 'Argosfilter'. Version 0.70. http://cran.at.r-project.org/web/packages/argosfilter/argosfilter.pdf

Furness RW, Wade HM, Masden EA (2013) Assessing vulnerability of marine bird populations to offshore wind farms. J Environ Manage 119:56–66

Gall AE, Morgan TC, Day RH, Kuletz KJ (2017) Ecological shift from piscivorous to planktivorous seabirds in the Chukchi Sea, 1975–2012. Polar Biol 40:61–78

Gall AE, Prichard AK, Kuletz KJ, Danielson SL (2022) Long: influence of water masses on the summer structure of the seabird community in the northeastern Chukchi Sea. PLOS ONE 17:e0266182

Garthe S, Hüppop O (2004) Scaling possible adverse effects of marine wind farms on seabirds: developing and applying a vulnerability index. J Appl Ecol 41:724–734

Gibble CM, Hoover BA (2018) Interactions between seabirds and harmful algal blooms. In: Shumway SE, Burkholder JM, Morton SL (eds) Harmful algal blooms: a compendium desk reference. John Wiley & Sons, Hoboken, NJ, p 223–242

Gilg O, Yoccoz NG (2010) Explaining bird migration. Science 327:276–277

Gill RE Jr, Handel CM (1981) Shorebirds of the eastern Bering Sea. In: Hood DW, Calder JA (eds) The eastern Bering Sea shelf: oceanography and resources, Vol 2. University of Washington Press, Seattle, WA, p 719–738

Gjerdrum C, Ronconi RA, Turner KL, Hamer TE (2021) Bird strandings and bright lights at coastal and offshore industrial sites in Atlantic Canada. Avian Conserv Ecol 16:22

Glibert PM, Allen JI, Artioli Y, Beusen A and others (2014) Vulnerability of coastal ecosystems to changes in harmful algal bloom distribution in response to climate change: projections based on model analysis. Glob Change Biol 20:3845–3858

Gradinger R (2009) Sea-ice algae: major contributors to primary production and algal biomass in the Chukchi and Beaufort Seas during May/June 2002. Deep Sea Res II 56: 1201–1212

Gratto-Trevor CL, Johnston VH, Pepper ST (1998) Changes in shorebird and eider abundance in the Rasmussen Lowlands, NWT. Wilson Bull 110:316–325

Grebmeier JM, Harrison NM (1992) Seabird feeding on benthic amphipods facilitated by gray whale activity in the northern Bering Sea. Mar Ecol Prog Ser 80:125–133

Grebmeier JM, Overland JE, Moore SE, Farley EV and others (2006) A major ecosystem shift in the northern Bering Sea. Science 311:1461–1464

Haney JC (1985) Wintering phalaropes off the southeastern United States: application of remote sensing imagery to seabird habitat analysis at oceanic fronts. J Field Ornithol 56:321–333

Harrison CS (1979) The association of marine birds and feeding gray whales. Condor 81:93–95

Harrison AL, Woodard PF, Mallory ML, Rausch J (2022) Sympatrically breeding congeneric seabirds (*Stercorarius* spp.) from Arctic Canada migrate to four oceans. Ecol Evol 12:e8451

Hays GC, Bailey H, Bograd SJ, Bowen WD and others (2019) Translating marine animal tracking data into conservation policy and management. Trends Ecol Evol 34:459–473

Herrera CM (1978) On the breeding distribution pattern of European migrant birds: MacArthur's theme reexamined. Auk 95:496–509

Hodgkins R (2014) The twenty-first century Arctic environment: accelerating change in the atmospheric, oceanic and terrestrial spheres. Geogr J 180:429–436

Holland MM, Bitz CM, Tremblay B (2006) Future abrupt reductions in the summer Arctic sea ice. Geophys Res Lett 33:L23503

Hop H, Vihtakari M, Bluhm BA, Daase M, Gradinger R, Melnikov IA (2021) Ice-associated amphipods in a pan-Arctic scenario of declining sea ice. Front Mar Sci 8:743152

Hopcroft R, Bluhm B, Gradinger R (eds) (2008) Arctic Ocean synthesis: analysis of climate change impacts in the Chukchi and Beaufort seas with strategies for future research. Institute of Marine Sciences, University of Alaska, Fairbanks, AK

Hu C, Lee Z, Franz B (2012) Chlorophyll *a* algorithms for oligotrophic oceans: a novel approach based on three-band reflectance difference. J Geophys Res 117:C01011

Humphries GRW, Huettmann F (2014) Putting models to a good use: a rapid assessment of Arctic seabird biodiversity indicates potential conflicts with shipping lanes and human activity. Divers Distrib 20:478–490

Hunnewell RW, Diamond AW, Brown SC (2016) Estimating the migratory stopover abundance of phalaropes in the outer Bay of Fundy, Canada. Avian Conserv Ecol 11:11

Hunt GL Jr, Stabeno P, Walters G, Sinclair E, Brodeur RD, Napp JM, Bond NA (2002) Climate change and control of the southeastern Bering Sea pelagic ecosystem. Deep Sea Res II 49:5821–5853

Hunt GL Jr, Coyle KO, Eisner LB, Farley EV and others (2011) Climate impacts on eastern Bering Sea foodwebs: a synthesis of new data and an assessment of the Oscillating Control Hypothesis. ICES J Mar Sci 68:1230–1243

Hunt GL Jr, Renner M, Kuletz K (2014) Seasonal variation in the cross-shelf distribution of seabirds in the southeastern Bering Sea. Deep Sea Res II 109:266–281

Huntington HP, Danielson SL, Wiese FK, Baker M and others (2020) Evidence suggests potential transformation of the Pacific Arctic ecosystem is underway. Nat Clim Chang 10:342– 348

Hyrenbach KD, Forney KA, Dayton PK (2000) Marine protected areas and ocean basin management. Aquat Conserv 10:437–458

Iken K, Bluhm B, Dunton K (2010) Benthic food-web structure under differing water mass properties in the southern Chukchi Sea. Deep Sea Res II 57:71–85

Johannessen OM, Bengtsson L, Miles MW, Kuzmina SI and others (2004) Arctic climate change: observed and modelled temperature and sea-ice variability. Tellus A Dyn Meterol Oceanogr 56:328–341

Jones T, Parrish JK, Peterson WT, Bjorkstedt EP and others (2018) Massive mortality of a planktivorous seabird in response to a marine heatwave. Geophys Res Lett 45: 3193–3202

Jones T, Parrish JK, Lindsey J, Wright C and others (2023) Marine bird mass mortality events as an indicator of the impacts of ocean warming. Mar Ecol Prog Ser: HEATav8

Jonsen ID, Patterson TA (2020) foieGras: Fit latent variable movement models to animal tracking data for location quality control and behavioural inference. Zenodo. https://doi.org/10.5281/zenodo.3899972

Jonsen ID, McMahon CR, Patterson TA, Auger-Méthé M, Harcourt R, Hindell MA, Bestley S (2019) Movement responses to environment: fast inference of variation among southern elephant seals with a mixed effects model. Ecology 100:e02566

Jonsen ID, Patterson TA, Costa DP, Doherty PD and others (2020) A continuous-time state-space model for rapid quality control of Argos locations from animal-borne tags. Mov Ecol 8:31

JPL MUR MEaSUREs Project (2015) GHRSST Level 4 MUR Global Foundation sea surface temperature analysis, v4.1. NASA Physical Oceanography Distributed Active Archive Center (PO.DAAC), Pasadena, CA (accessed 21 Dec 2021)

Krietsch J, Cragnolini M, Kuhn S, Lanctot RB, Saalfeld ST, Valcu M, Kempenaers B (2022) Extrapair paternity in a sequentially polyandrous shorebird: limited evidence for the sperm storage hypothesis. Anim Behav 183:77–92

Kuletz KJ, Labunski EA (2017) Seabird distribution and abundance in the offshore environment, final report. OCS Study BOEM 2017-004. US Fish and Wildlife Service and Bureau of Ocean Energy Management, US Department of the Interior, Anchorage, AK

Kuletz KJ, Ferguson MC, Hurley B, Gall AE, Labunski EA, Morgan TC (2015) Seasonal spatial patterns in seabird and marine mammal distribution in the eastern Chukchi and western Beaufort seas: identifying biologically important pelagic areas. Prog Oceanogr 136:175–200

Kuletz KJ, Cushing DA, Osnas EE, Labunski EA, Gall AE (2019) Representation of the Pacific Arctic seabird community within the Distributed Biological Observatory array, 2007–2015. Deep Sea Res Part II 162:191–210

Kuletz K, Cushing D, Labunski E (2020) Distributional shifts among seabird communities of the northern Bering and Chukchi seas in response to ocean warming during 2017–2019. Deep Sea Res Part II 181–182:104913

Kumlien L (1879) Contributions to the natural history of Arctic America, made in connection with the Howgate Polar Expedition, 1877–78. Bull U S Natl Mus 15

Ladd C, Jahncke J, Hunt GL Jr, Coyle KO, Stabeno PJ (2005) Hydrographic features and seabird foraging in Aleutian Passes. Fish Oceanogr 14:178–195

Lebreton L, Slat B, Ferrari F, Sainte-Rose B and others (2018) Evidence that the Great Pacific Garbage Patch is rapidly accumulating plastic. Sci Rep 8:4666

Levine RM, De Robertis A, Grünbaum D, Wildes S, Farley EV, Stabeno PJ, Wilson CD (2023) Climate-driven shifts in pelagic fish distributions in a rapidly changing Pacific Arctic. Deep Sea Res II 208:105244

Liebezeit JR, Smith PA, Lanctot RB, Schekkerman H and others (2007) Assessing the development of shorebird eggs using the flotation method: species-specific and generalized regression models. Condor 109:32–47

Lopez R, Malardé JP, Royer F, Gaspar P (2014) Improving Argos doppler location using multiple-model Kalman filtering. IEEE Trans Geosci Remote Sens 52:4744–4755

Macias-Fauria M, Post E (2018) Effects of sea ice on Arctic biota: an emerging crisis discipline. Biol Lett 14:20170702

Maftei M, Davis SE, Mallory ML (2015) Confirmation of a wintering ground of Ross's gull *Rhodostethia rosea* in the northern Labrador Sea. Ibis 157:642–647

Mayfield HF (1975) Suggestions for calculating nest success. Wilson Bull 87:456–466

McKinnon L, Smith PA, Nol E, Martin JL and others (2010) Lower predation risk for migratory birds at high latitudes. Science 327:326–327

Meissner T, Wentz FJ, Le Vine DM (2018) The salinity retrieval algorithms for the NASA Aquarius version 5 and SMAP version 3 releases. Remote Sens 10:1121

Meissner T, Wentz FJ, Manaster A, Lindsley R (2019) Remote sensing systems SMAP ocean surface salinities [Level 3 monthly], version 4.0 validated release. Remote Sensing Systems, Santa Rosa, CA. doi:10.5067/SMP40-3SMCS (accessed 19 Dec 2021)

Merkel FR (2010) Light-induced bird strikes on vessels in southwest Greenland. Technical Report No. 84. Pinngortitaleriffik, Greenland Institute of Natural Resources, Nuuk

Michelot T, Langrock R (2019) A short guide to choosing initial parameter values for the estimation in moveHMM: an R vinaigrette. https://cran.r-project.org/web/packages/moveHMM/vignettes/moveHMM-starting-values.pdf

Michelot T, Langrock R, Patterson TA (2016) moveHMM: an R package for the statistical modelling of animal movement data using hidden Markov models. Methods Ecol Evol 7:1308–1315

Moore SE (2016) Is it 'boom times' for baleen whales in the Pacific Arctic region? Biol Lett 12:20160251

Moore CJ, Moore SL, Leecaster MK, Weisberg SB (2001) A comparison of plastic and plankton in the North Pacific central gyre. Mar Pollut Bull 42:1297–1300

Moore SE, Grebmeier JM, Davies JR (2003) Gray whale distribution relative to forage habitat in the northern Bering Sea: current conditions and retrospective summary. Can J Zool 81:734–742

Mordy CW, Stabeno PJ, Ladd C, Zeeman S, Wisegarver DP, Salo SA, Hunt GL Jr (2005) Nutrients and primary production along the eastern Aleutian Island Archipelago. Fish Oceanogr 14:55–76

Moser ML, Lee DS (1992) A fourteen-year survey of plastic ingestion by western north Atlantic seabirds. Colon Waterbirds 15:83–94

Mueter FJ, Iken K, Cooper LW, Grebmeier JM and others (2021) Changes in diversity and species composition across multiple assemblages in the eastern Chukchi Sea during two contrasting years are consistent with borealization. Oceanography 34:38–51

NASA Goddard Space Flight Center, Ocean Ecology Laboratory, Ocean Biology Processing Group (2018) Moderate-resolution imaging spectroradiometer (MODIS) aqua chlorophyll data; 2018 Reprocessing. NASA Ocean Biology Distributed Active Archive Center (OB.DAAC), Greenbelt, MD, doi:10.5067/AQUA/MODIS/L3M/CHL/2018 (accessed 8 Dec 2021)

NASA Ocean Biology Processing Group and R.P. Stumpf (2012) Distance to nearest coastline: 0.04-degree grid. https://oceancolor.gsfc.nasa.gov/docs/distfromcoast/ (accessed 17 Dec 2021)

Nelson EW (1883) The birds of Bering Sea and the Arctic Ocean. In: Cruise of the revenue-steamer Corwin in Alaska and the NW Arctic Ocean in 1881: notes and memoranda, medical and anthropological, botanical, ornithological. Government Printing Office, Washington, DC, p 57–118

Nevitt GA (2008) Sensory ecology on the high seas: the odor world of the procellariiform seabirds. J Exp Biol 211:1706–1713

Newton I (2008) The migration ecology of birds. Academic Press, London
Newton I (2012) Obligate and facultative migration in birds: ecological aspects. J Ornithol 153:171–180
Newton I, Dale L (1996) Relationship between migration and latitude among west European birds. J Anim Ecol 65: 137–146
Notz D, Stroeve J (2016) Observed Arctic sea-ice loss directly follows anthropogenic CO_2 emission. Science 354:747–750
O'Hara PD, Morandin LA (2010) Effects of sheens associated with offshore oil and gas development on the feather microstructure of pelagic seabirds. Mar Pollut Bull 60: 672–678
Obst BS, Hunt GL Jr (1990) Marine birds feed at gray whale mud plumes in the Bering Sea. Auk 107:678–688
Orr CD, Ward RMP, Williams NA, Brown RGB (1982) Migration patterns of red and northern phalaropes in southwest Davis Strait and in the northern Labrador Sea. Wilson Bull 94:303–312
Overland JE, Stabeno PJ (2004) Is the climate of the Bering Sea warming and affecting the ecosystem? EOS Trans AGU 85:309–312
Overland JE, Wang M (2013) When will summer Arctic be nearly sea ice free? Geophys Res Lett 40:2097–2101
Palacios DM, Bograd SJ, Foley DG, Schwing FB (2006) Oceanographic characteristics of biological hot spots in the North Pacific: a remote sensing perspective. Deep Sea Res II 53:250–269
Park J, Lee S, Jo YH, Kim HC (2021) Phytoplankton bloom changes under extreme geophysical conditions in the northern Bering Sea and the southern Chukchi Sea. Remote Sens 13:4035
Piatt JF, Springer AM (2003) Advection, pelagic food webs and the biogeography of seabirds in Beringia. Mar Ornithol 31:141–154
Pickart RS, Schulze LM, Moore GWK, Charette MA, Arrigo KR, van Dijken G, Danielson SL (2013) Long-term trends of upwelling and impacts on primary productivity in the Alaskan Beaufort Sea. Deep Sea Res I 79:106–121
Pidwirny M (2006) Surface and subsurface ocean currents: ocean current map. Fundamentals of physical geography, 2nd edn. www.physicalgeography.net/fundamentals/8q_1.html (accessed 17 Mar 2022)
Piersma T (1997) Do global patterns of habitat use and migration strategies co-evolve with relative investments in immunocompetence due to spatial variation in parasite pressure? Oikos 80:623–631
Pisareva MN, Pickart RS, Lin P, Fratantoni PS, Weingartner TJ (2019) On the nature of wind-forced upwelling in Barrow Canyon. Deep Sea Res II 162:63–78
Priklonsky SG (1960) Application of small automatic bows for catching birds. Zool Zh 39:623–624
R Core Team (2021) R: a language and environment for statistical computing. R Foundation for Statistical Computing, Vienna
Romano MD, Renner HM, Kuletz KJ, Parrish JK and others (2020) Die-offs, reproductive failure, and changing at-sea abundance of murres in the Bering and Chukchi seas in 2018. Deep Sea Res II 181-182:104877
Saalfeld ST, Lanctot RB (2015) Conservative and opportunistic settlement strategies in Arctic-breeding shorebirds. Auk 132:212–234
Saalfeld ST, Lanctot RB, Brown SC, Saalfeld DT, Johnson JA, Andres BA, Bart JR (2013) Predicting breeding shorebird distributions on the Arctic Coastal Plain of Alaska. Ecosphere 4:16
Sambrotto RN, Goering JJ, McRoy CP (1984) Large yearly production of phytoplankton in the western Bering Strait. Science 225:1147–1150
Schneider D (1982) Fronts and seabird aggregations in the southeastern Bering Sea. Mar Ecol Prog Ser 10:101–103
Serreze MC, Francis JA (2006) The Arctic amplification debate. Clim Change 76:241–264
Seyer Y, Gauthier G, Bêty J, Therrien JF, Lecomte N (2021) Seasonal variations in migration strategy of a long-distance Arctic-breeding seabird. Mar Ecol Prog Ser 677:1–16
Sigler MF, Napp JM, Stabeno PJ, Heintz RA, Lomas MW, Hunt GL Jr (2016) Variation in annual production of copepods, euphausiids, and juvenile walleye pollock in the southeastern Bering Sea. Deep Sea Res II 134: 223–234
Silber GK, Weller DW, Reeves RR, Adams JD, Moore TJ (2021) Co-occurrence of gray whales and vessel traffic in the North Pacific Ocean. Endang Species Res 44: 177–201
Sittler B, Aebischer A, Gilg O (2011) Post-breeding migration of four long-tailed skuas (*Stercorarius longicaudus*) from north and east Greenland to West Africa. J Ornithol 152: 375–381
Smith KG, Connors PG (1993) Postbreeding habitat selection by shorebirds, water birds, and land birds at Barrow, Alaska: a multivariate analysis. Can J Zool 71:1629–1638
Smith MA, Walker NJ, Free CM, Kirchhoff MJ, Drew GS, Warnock N, Stenhouse IJ (2014) Identifying marine Important Bird Areas using at-sea survey data. Biol Conserv 172:180–189
Smith MA, Goldman MS, Knight EJ, Warrenchuk JJ (2017) Ecological atlas of Bering, Chukchi, and Beaufort seas, 2nd edn. Audubon Alaska, Anchorage, AK
Smith PA, McKinnon L, Meltofte H, Lanctot RB and others (2020) Status and trends of tundra birds across the circumpolar Arctic. Ambio 49:732–748
Somveille M, Rodrigues ASL, Manica A (2015) Why do birds migrate? A macroecological perspective. Glob Ecol Biogeogr 24:664–674
Spreen G, Kaleschke L, Heygster G (2008) Sea ice remote sensing using AMSR-E 89 GHz channels. J Geophys Res 113:C02S03
Springer AM, McRoy CP, Flint MV (1996) The Bering Sea Green Belt: shelf-edge processes and ecosystem production. Fish Oceanogr 5:205–223
Stafford KM, Farley EV, Ferguson M, Kuletz KJ, Levine R (2022) Northward range expansion of subarctic upper trophic level animals into the Pacific Arctic region. Oceanography 35:158–166
Stevenson DE, Lauth RR (2019) Bottom trawl surveys in the northern Bering Sea indicate recent shifts in the distribution of marine species. Polar Biol 42:407–421
Stienen EWM, Waeyenberge V, Kuijken E, Seys J (2007) Trapped within the corridor of the southern North Sea: the potential impact of offshore wind farms on seabirds. In: de Lucas M, Janss GEE, Ferrer M (eds) Birds and wind farms: risk assessment and mitigation. Quercus, Madrid, p 71–80
Stroeve J, Notz D (2018) Changing state of Arctic sea ice across all seasons. Environ Res Lett 13:103001
Strong C, Rigor IG (2013) Arctic marginal ice zone trending wider in summer and narrower in winter. Geophys Res Lett 40:4864–4868

Taylor AR, Lanctot RB, Powell AN, Huettmann F, Nigro DA, Kendall SJ (2010) Distribution and community characteristics of staging shorebirds on the northern coast of Alaska. Arctic 63:451–467

Taylor AR, Lanctot RB, Powell AN, Kendall SJ, Nigro DA (2011) Residence time and movements of postbreeding shorebirds on the northern coast of Alaska. Condor 113:779–794

Thaxter CB, Ross-Smith VH, Clark JA, Clark NA and others (2016) Contrasting effects of GPS device and harness attachment on adult survival of lesser black-backed gulls *Larus fuscus* and great skuas *Stercorarius skua.* Ibis 158: 279–290

Timmermans ML, Labe Z (2020) Sea surface temperature. In: Thoman RL, Richter-Menge J, Druckenmiller ML (eds) Arctic Report Card 2020. https://doi.org/10.25923/v0fs-m920

Tracy DM, Schamel D, Dale J (2020) Red phalarope (*Phalaropus fulicarius*), version 1.0. In: Billerman SM (ed) Birds of the world. Cornell Lab of Ornithology, Ithaca, NY

Tsujii K, Otsuki M, Akamatsu T, Amakasu K and others (2021) Annual variation of oceanographic conditions changed migration timing of bowhead whales *Balaena mysticetus* in the southern Chukchi Sea. Polar Biol 44:2289–2298

Tyler WB, Briggs KT, Lewis DB, Ford RG (1993) Seabird distribution and abundance in relation to oceanographic processes in the California Current system. In: Vermeer K, Briggs KT, Morgan KH, Siegal-Causey D (eds) The status, ecology, and conservation of marine birds of the North Pacific. Canadian Wildlife Service, Environment Canada, Ottawa, p 48–60

US National Ice Center (2020) US National Ice Center daily marginal ice zone products, version 1. National Snow and Ice Data Center (NSIDC), Boulder, CO (accessed 14 Feb 2022)

van Bemmelen RSA (2019) Seabirds linking Arctic and ocean. PhD dissertation, Wageningen University

Van Hemert C, Schoen SK, Litaker RW, Smith MM and others (2020) Algal toxins in Alaskan seabirds: evaluating the role of saxitoxin and domoic acid in a large-scale die-off of common murres. Harmful Algae 92:101730

Van Hemert C, Dusek RJ, Smith MM, Kaler R and others (2021) Investigation of algal toxins in a multispecies seabird die-off in the Bering and Chukchi seas. J Wildl Dis 57:399–407

Vermeer K, Briggs KT, Morgan KH, Siegal-Causey D (eds) (1993) The status, ecology, and conservation of marine birds of the North Pacific. Canadian Wildlife Service, Environment Canada, Ottawa

Wahl TR, Morgan KH, Vermeer K (1993) Seabird distribution off British Columbia and Washington. In: Vermeer K, Briggs KT, Morgan KH, Siegal-Causey D (eds) The status, ecology, and conservation of marine birds of the North Pacific. Canadian Wildlife Service, Environment Canada, Ottawa, p 39–47

Wang M, Overland JE (2009) A sea ice free summer Arctic within 30 years? Geophys Res Lett 36:L07502

Wang M, Yang Q, Overland JE, Stabeno P (2018) Sea-ice cover timing in the Pacific Arctic: the present and projections to mid-century by selected CMIP5 models. Deep Sea Res II 152:22–34

Warnock N, Warnock S (1993) Attachment of radio-transmitters to sandpipers: review and methods. Wader Study Group Bull 70:28–30

Webb EE, Liljedahl AK, Cordeiro JA, Loranty MM, Witharana C, Lichstein JW (2022) Permafrost thaw drives surface water decline across lake-rich regions of the Arctic. Nat Clim Chang 12:841–846

Weimerskirch H (2007) Are seabirds foraging for unpredictable resources? Deep Sea Res II 54:211–223

Weiser EL, Lanctot RB, Brown SC, Gates HR and others (2018a) Environmental and ecological conditions at Arctic breeding sites have limited effects on true survival rates of adult shorebirds. Auk 135:29–43

Weiser EL, Brown SC, Lanctot RB, Gates HR and others (2018b) Life-history tradeoffs revealed by seasonal declines in reproductive traits of Arctic-breeding shorebirds. J Avian Biol 49:e01531

Will A, Takahashi A, Thiebot JB, Martinez A and others (2020) The breeding seabird community reveals that recent sea ice loss in the Pacific Arctic does not benefit piscivores and is detrimental to planktivores. Deep Sea Res II 181–182:104902

Winker K, Gibson DD, Sowls AL, Lawhead BE, Martin PD, Hoberg EP, Causey D (2002) The birds of St. Matthew Island, Bering Sea. Wilson Bull 114:491–509

Zhang X, Walsh JE (2006) Toward a seasonally ice-covered Arctic Ocean: scenarios from the IPCC AR4 model simulations. J Clim 19:1730–1747

Appendix A. Full author addresses

Sarah T. Saalfeld[1], Mihai Valcu[2], Stephen Brown[3], Willow English[4], Marie-Andrée Giroux[5], Autumn-Lynn Harrison[6], Johannes Krietsch[2], Kathy Kuletz[1], Jean-François Lamarre[7], Christopher Latty[8], Nicolas Lecomte[9], Rebecca McGuire[10], Martin Robards[10], Amy Scarpignato[6], Shiloh Schulte[3], Paul A. Smith[11], Bart Kempenaers[2], Richard B. Lanctot[1]

[1]Migratory Bird Management Division, US Fish and Wildlife Service, Anchorage, Alaska 99503, USA
[2]Department of Ornithology, Max Planck Institute for Biological Intelligence, 82319 Seewiesen, Germany
[3]Manomet Inc., Manomet, Massachusetts 02345, USA
[4]Department of Biology, Carleton University, Ottawa, Ontario K1S 5B6, Canada
[5]K.-C.-Irving Research Chair in Environmental Sciences and Sustainable Development, Département de Chimie et de Biochimie, Université de Moncton, Moncton, New Brunswick E1A 3E9, Canada
[6]Migratory Bird Center, Smithsonian's National Zoo & Conservation Biology Institute, Washington, DC 20008, USA
[7]Canadian High Arctic Research Station (CHARS), Polar Knowledge Canada, Cambridge Bay, Nunavut X0B 0C0, Canada
[8]Arctic National Wildlife Refuge, US Fish and Wildlife Service, Fairbanks, Alaska 99701, USA
[9]Canada Research Chair in Polar and Boreal Ecology and Centre d'Études Nordiques, Department of Biology, Université de Moncton, Moncton, New Brunswick E1A 3E9, Canada
[10]Arctic Beringia Program, Wildlife Conservation Society, Fairbanks, Alaska 99709, USA
[11]Wildlife Research Division, Environment and Climate Change Canada, National Wildlife Research Centre, Ottawa, Ontario K1A 0H3, Canada

Appendix B. Individual red phalarope travel distances in relation to hypothetical migration route

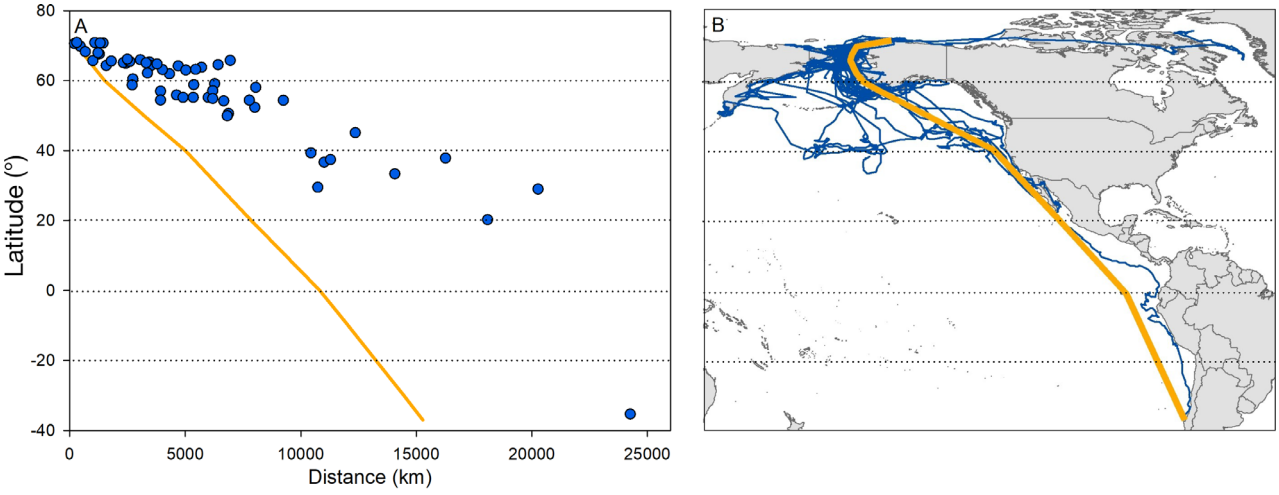

Figure A1. (A) total distance traveled (blue dots) by post-breeding red phalaropes (i.e. distance from last breeding site to an individual's wintering area or to last migration location) in relation to an individual's most southerly latitude (i.e. minimum latitude) from 2017–2020. For comparison, distances traveled by latitude along a hypothetical migration route are displayed (orange line). The hypothetical migration route was created to show the minimum travel distance while maintaining the general migration pattern. (B) Individual migration routes of red phalaropes during southward migration (blue lines) and the hypothetical migration route (orange line). Predicted red phalarope locations were generated every 8 h for individuals using continuous-time random walk state-space models and were restricted to individuals captured at Utqiaġvik, Alaska, where the majority of birds were tagged

Editorial responsibility: Thierry Boulinier, Montpellier, France
Reviewed by: 2 anonymous referees

Submitted: January 30, 2023
Accepted: January 8, 2024
Proofs received from author(s): February 19, 2024